Spatial mRNA profiling using Rapid Amplified Multiplexed-FISH (RAM-FISH)

Tirtha Das Banerjee[1,*], Joshua Raine[2], Ajay S. Mathuru[2,3,4], Kok Hao Chen[5], Antónia Monteiro[1,*]

Affiliations

[1]Department of Biological Sciences, National University of Singapore 117557, Singapore.

[2] Department of Physiology, Yong Loo Lin School of Medicine, National University of Singapore, Singapore.

[3] Institute for Digital Medicine (WisDM), Yong Loo Lin School of Medicine, National University of Singapore, Singapore

[4] Healthy Longevity TRP, Yong Loo Lin School of Medicine, National University of Singapore, Singapore

[5] Genome Institute of Singapore, Agency for Science, Technology and Research (A*STAR), Singapore.

*Authors for correspondence: tirtha_banerjee@u.nus.edu; antonia.monteiro@nus.edu.sg

Abstract

Localizing multiple RNA molecules simultaneously in intact tissues and organs is valuable for gaining insights into possible gene-regulatory interactions underlying cell differentiation. Existing technologies for multiplexed RNA localization are expensive, computationally complex, have elaborate sample preparation steps, have size limitations, and require weeks of processing time. This limits the widespread use of such techniques in most labs. Here we describe a cost-effective methodology, Rapid Amplified Multiplexed-FISH (or RAM-FISH), based on Hybridization Chain Reaction 3.0 for localizing dozens of transcripts in the same sample. This methodology achieves multiplexing by localizing 3 genes per cycle to detect 30 or more genes within a few days. The method can be applied to fixed tissue sections, entire organs, or whole organisms such as larval *Danio rerio*, without extensive sample preparation steps. The automation used here can also be adapted to perform other amplification-based FISH. Here, we demonstrate its utility, flexibility, and versatility for gene expression analysis in two very different types of samples, *Bicyclus anynana* butterfly larval wings and intact 10-day-old *Danio rerio* fish larvae.

Keywords

Multiplex-FISH, HCR3.0, *Bicyclus anynana*, *Danio rerio*, RAM-FISH.

Introduction

Multicellular lifeforms are complex systems controlled by dynamic spatial and temporal patterns of gene expression. These gene expression dynamics can be visualized via the detection of RNA molecules in cells. Many biologists are therefore interested in simple, robust methodologies for the simultaneous detection of multiple RNA molecules in intact tissues. This detection can be used to describe natural tissue differentiation, initiation of disease pathologies, or, when combined with CRISPR-Cas9, used to describe the architecture of gene-regulatory networks. These investigations demand a robust and expedient method combining high signal specificity and sensitivity while reducing human labor and errors. In addition, reduced requirements for extensive sample preparation, and increased applicability to diverse sample types are also desirable features for RNA localization methodologies.

Recent technological advancements enable single-cell RNA expression profiling while preserving tissue architecture. These methods can be categorized into two primary types: sequencing-based and imaging-based using fluorescently-tagged probes for RNA signal quantification. The first includes platforms such as Visium (Ståhl et al., 2016), Stereo-seq (Chen et al., 2022), and Slide-seq (Rodriques et al., 2019). The second includes imaging-based technologies MERFISH (Chen et al., 2015), osmFISH (Codeluppi et al., 2018), CosMx SMI (He et al., 2021), STARmap (Wang et al., 2018), seq-FISH (Lubeck and Cai, 2012), , and FISH&CHIPS (Zhou et al., 2023a). While these methods are valuable, challenges such as complex tissue preparation steps, high costs, complex setups, and the potential for false positives and background noise can pose a challenge for some samples.

The development of signal amplification and background suppression methods has provided alternatives to these existing methodologies. Methods such as HCR3.0 (Choi et al., 2018; Schulte et al., 2024), SABER-FISH (Kishi et al., 2019), split-FISH (Goh et al., 2020), and RNAScope (Wang et al., 2012) provide signal amplification and use split probes to reduce background signals. Despite these significant improvements, these technologies still face some limitations, including 1) limited multiplexing capacity, 2) lengthy experimental timelines, and 3) labor-intensive protocols requiring specialized training and manual sample handling, which can introduce errors. HCR3.0 based technologies such as cycleHCR (Gandin et al., 2024) and EASI-FISH (Wang et al., 2021) have overcome the limited multiplexing capacity, however, with the limitation of complex experimental setups and computationally challenging data processing which still remains out of reach for many labs.

Here, we present RAM-FISH, a Hybridization Chain Reaction (HCR3.0) (Choi et al., 2018) based method, coupled with multiplexing, and automation, to efficiently detect 30 or more target genes through multiple rounds of HCR on the same sample. We have previously employed this automation system and a single HCR round to characterize gene expression in *Bicyclus anynana* developing scales and intact *Danio rerio* larval brains (Prakash et al., 2024; Raine et al., 2024; Tian et al., 2024). Here, with RAM-FISH, we show multiplexing of this approach to multi-round HCR. This methodology is relatively simple, cost-effective, and capable of analyzing tissue sections, entire organs, and even whole organisms within a few days. The method can be carried out manually or using the automation system without direct confocal attachment.

Overview of the Workflow: Manual and using automation

The workflow involves the dissection or collection of tissues (**Figure 1A)**, followed by fixing and permeabilization (**Figure 1B**). Afterwards, the tissue samples are either tested manually (**Figure 1C and D**) or using the automation system (**Figure 1E and F**).

For the free-floating manual protocol, the hybridization, washes, and signal removal steps are carried out in glass spot plates or 1.5 ml centrifuge tubes (**Figure 1C**). For the gel-based methodology, the samples are embedded in acrylamide-based gel in a 3.5 cm confocal dish. Hybridization and washes are carried out in the dish and subsequently imaged. The signals are then removed in the same dish (**Figure 1D**), and the process repeated multiple times. The different channels are merged to obtain a multiplexed tissue image.

For the automation protocol, samples are treated either in a free-floating environment (**Figure 1E**) or in a gel-based environment (**Figure 1F**). In the free-floating protocol, tissue samples are placed in a microcomb holder (**Figure 1E,** part 1), and any additional fluids are removed followed by the installation of part 2 and an arc reaction chamber (**Figure 1E**). The reactions are performed in a fluidics automation system. Afterward, the samples are mounted in a slide with mounting media and imaged. Samples are afterward removed from the slide and returned to the microcomb for signal removal and repetition of the cycle (**Figure 1F)**. In the gel-based environment, the reactions are carried out in part 1 of the gel-specific microcomb followed by the installation of part 2 (**Figure 1F**). Afterwards, the remaining reactions are performed in the automation system followed by imaging of the sample in a 3.5 cm dish under a confocal microscope. After imaging, the signal is removed, samples are returned to the automation system, and the cycle is repeated (**Figure 1E, F**).

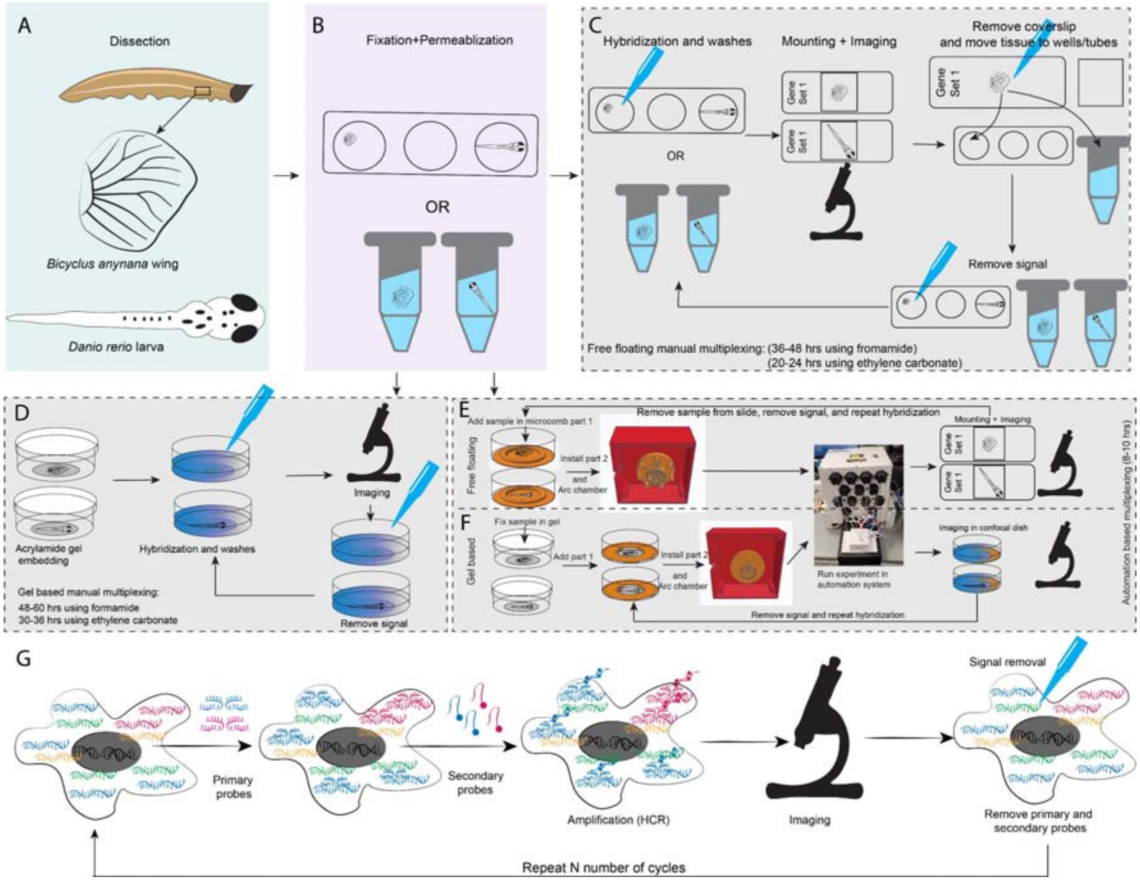
A
Dissection
Bicyclus anynana wing
Danio rerio larva
B
Fixation+Permeablization
OR
C
Hybridization and washes
Mounting + Imaging
Remove coverslip
and move tissue to wells/tubes
Gene Set 1
OR
Remove signal
Free floating manual multiplexing: (36-48 hrs using fromamide)
(20-24 hrs using ethylene carbonate)
D
Acrylamide gel embedding
Hybridization and washes
Imaging
Remove signal
Gel based manual multiplexing:
48-60 hrs using formamide
30-36 hrs using ethylene carbonate
E
Remove sample from slide, remove signal, and repeat hybridization
Add sample in microcomb part 1
Free floating
Install part 2
and
Arc chamber
Mounting + Imaging
Gene Set 1
F
Fix sample in gel
Gel based
Add part 1
Install part 2
and
Arc chamber
Run experiment in automation system
Imaging in confocal dish
Remove signal and repeat hybridization
Automation based multiplexing (8-10 hrs)
G
Primary probes
Secondary probes
Amplification (HCR)
Imaging
Signal removal
Remove primary and secondary probes
Repeat N number of cycles

Figure 1: Illustration of the manual and the automation-based multiplexing protocol. (**A**) Tissues are dissected, fixed, and permeabilized in glass spot plates or 1.5ml microcentrifuge plates. Afterwards, multiplexing can be performed either manually (**B, C**), or using an automation system (**D, E**). (**F**) An illustration of the reactions where primary probes bind to the target mRNA of interest, followed by amplification using secondary probes via HCR3.0. Imaging is conducted under a confocal microscope followed by the removal of primary and secondary probes. The steps are repeated multiple times.

Probes preparation

To aid the probe design process we produced two excel-based sheets. The first sheet (CDS_gene_extractor.xml) extracts 25 bps nucleotides for both the forward and reverse strand of the chosen HCR primary probe binding sites and reverse complements them. The second sheet (Amplifier_adder.xml) adds the amplifiers specific against the selected pairs of complementary sites. Briefly, a candidate gene coding sequence file from a repository such as ncbi (https://ncbi.nlm.nih.gov/) was downloaded and copy-pasted in the first column of the CDS_gene_extractor file. A reverse complement macro (https://github.com/LJI-Bioinformatics/Excel-Reverse-Complement) was loaded to the excel sheet. This produces 25 bp pairs of nucleotides which were copied and pasted to the amplifier_adder file which has the secondary fluorescent specific amplifier sequence. All the probe sequences used in the present work along with the gene CDS are provided in the **supplementary file 2**.

Imaging multiple genes on developing butterfly wing (Stages 0.75-3.25)

The manual multiplexing methodology was used to investigate the expression patterns of multiple genes on the developing larval wings of *Bicyclus anynana* butterflies. Many of these genes play important functions in the development of distinct colour patterns observed in the adults (**Figure S1**). During the larval stages, gene expression patterns are highly complex and dynamic (Banerjee et al., 2023; Connahs et al., 2019a). We tested the expression of 33 known and novel genes during different developmental stages from 0.75-3.25 (staging of wings are described in (Banerjee and Monteiro, 2020a; Reed et al., 2007)) to explore expression dynamics, and carried over 10-14 rounds of hybridization and washes (**Figure 3-6; Figure S3-S6**). Many of these genes have been previously studied using immunofluorescence and *in-situ* hybridization, and functionally tested using CRISPR-Cas9 and RNAi (**Table S1**). Below we provide a brief description of the expression pattern of each of the genes and describe whether the expression is consistent with previous findings in this or other butterfly species or is newly described for butterflies. The coding sequences and the probes used for the detection of the genes are provided in the **supplementary file 2**.

1) *Wnt1* was expressed along the wing margin and along the discal spots, overlapping the expression patterns of *Wnt10* and *Wnt6*, consistent with previous findings (Banerjee and Monteiro, 2020a; Banerjee et al., 2023; Martin and Reed, 2014) (**Figure 2A, Figure 3A, Figure 4A, Figure 5A, Figure 6A, Figure S3-S6**).

2) *Wnt6* was expressed along the wing margin and in the discal spots of butterflies consistent with previous findings (Banerjee et al., 2023; Martin and Reed, 2014) (**Figure 2B, Figure 3B, Figure 4B, Figure 5B, Figure 6B, Figure S3-S6**).

3) *Wnt10* was observed along the wing margin as well as in the discal spot consistent with previous findings (Banerjee et al., 2023; Martin and Reed, 2014) (**Figure 2C, Figure 3C, Figure 4C, Figure 6C, Figure S3-S6**).

4) *WntA* was expressed in bands along the central symmetry system and along the marginal band system consistent with previous studies (Banerjee et al., 2023; Hanly et al., 2023; Martin and Reed, 2014; Mazo-vargas et al., 2017) (**Figure 2D, Figure 3D, Figure 5C, Figure 6D, Figure S3-S6**).

5) *cubitus interruptus (ci)* was expressed in the anterior compartment of the developing wing discs and in the eyespot centers, consistent with the previous studies (Banerjee and Monteiro, 2023; Keys et al., 1999) (**Figure 2E, Figure 3E, Figure 4D, Figure 6E, Figure S3-S5**). We noticed a strong expression of *Ci* in M1 and a fainter expression in M2 eyespots, in hindwings at stage 2.5, whereas the remaining eyespots did not express *Ci* (**Figure 6E, Figure S6)**. This absence of *Ci* expression in eyespot centers positioned away from the anterior-posterior (AP) boundary of the wing is consistent with the finding from Reed et al., 2020.

6) *rhomboid (rho)* mRNA expression was visualized in the veins of butterflies consistent with previous protein expression results from butterflies (Banerjee and Monteiro, 2020a) and mRNA results from *Drosophila* (Guichard et al., 1999) (**Figure 2F, Figure 3F, Figure 4E, Figure S3-S6**).

7) *homothorax (hth)* expression was newly visualized along two bands along the proximal domain of the developing larval wings (**Figure 2G, Figure 3G, Figure 4F, Figure 6F, Figure S3-S6**). A previous study has looked at the expression of *hth* in the pupal wing (Hanly et al., 2019).

8) *aristaless (al/al1)* was expressed in the anterior compartment along a band running the proximal AP domain of the larval wings consistent with previous protein and mRNA expression patterns in different butterfly species (Banerjee and Monteiro, 2020a; Martin and Reed, 2010) (**Figure 2H, Figure 3H, Figure 4G, Figure 5D, Figure S3-S6**).

9) *frizzled2 (fz2)* was expressed in the proximal domain of the developing larval wing consistent with previous results in other butterfly species (Banerjee et al., 2023; Hanly et al., 2023) (**Figure 2I, Figure 3I, Figure 4H, Figure 6G, Figure S3-S6**).

10) *frizzled4 (fz4)* was expressed in the intervein cells during the early stages of development (stage 0.75-1.00) (**Figure 2J, Figure 3J, Figure 5E, Figure S3-S5**). During the later stages (2.50-3.25) *fz4* expression was observed in the intervein cells along with missing expression in the eyespot center (**Figure 4I, Figure 6H, Figure S6).** These results are consistent with results from previous findings (Banerjee et al., 2023).

11) *frizzled9/frizzled3 (fz9)* was expressed along the wing margin, consistent with previous findings (Banerjee et al., 2023; Hanly et al., 2023) (**Figure 2K, Figure 3K, Figure 4J, Figure 5F, Figure 6I, Figure S3-S6**).

12) *dachshund (dac)* was newly visualized in three distinct domains on the anterior compartment of the hindwing (stage 1.00 and 2.50) (**Figure 5G, Figure 6J, Figure S4, Figure S5)** and in an anterior proximal domain, with slightly higher expression in the lower posterior compartment on the forewing during wing development (**Figure 2L, Figure 3L, Figure S3, Figure S6**).

13) *thickvein (tkv)* was expressed around the intervein cells with stronger expression in cells distant from *dpp* expressing cells, consistent with previous findings in butterflies (Banerjee and Monteiro, 2023) and *Drosophila* (Funakoshi et al., 2001) (**Figure 2M, Figure 3M, Figure 5H, Figure 6K, Figure S3-S6**).

14) *mirror* was expressed in the lower posterior compartment of the developing larval wings consistent with a previous study (Chatterjee et al., 2024). Slightly higher expression of *mirror* was also observed in the proximal domain in the anterior compartment of the developing wings (**Figure 2N, Figure 3N, Figure 4K, Figure 5I, Figure S3-S6**).

15) *sister of odd and bowel (sob)* was newly visualized in a strong proximal band as well as at lower levels in a broad distal band (**Figure 2, Figure 3O, Figure 4L, Figure 5J, Figure S3-S6**).

16) *Distal-less (Dll)* was expressed along the wing margin with finger like projections during early wing development (Stages 0.75-1.00) (**Figure 2P, Figure 3P, Figure 5K, Figure S3-S5**). During the later stages, *Dll* expression was observed along the wing margin and in the eyespot centers (**Figure 6L, Figure S6).** These results are consistent with previous findings (Carroll et al. 1994; Brakefield et al. 1996; Banerjee et al., 2023; Connahs et al., 2019b; Reed and Gilbert, 2004; Reed et al., 2020; Shirai et al. 2012, Oliver et al. 2012; Wee et al., 2022).

17) *optomotor-blind (omb)* was expressed along a broad domain along the AP boundary as well as in the lower posterior compartment (**Figure 2Q, Figure 3Q, Figure 5L, Figure S3-S5**). During the later stages of development, expression in the eyespot centers was also observed (**Figure 4M, Figure 6M, Figure S6)**. These results are consistent with a previous finding (Banerjee and Monteiro, 2023).

18) *heat shock promoter 67b (hsp67b)* was newly visualized in complex and dynamic patterns in larval wings. Major expression domains were observed along the anterior compartment and in the wing margin (**Figure 2R, Figure 3R, Figure 4N, Figure S3-S6**).

19) *hedgehog (hh)* expression was observed in the posterior compartment, consistent with previous studies (Keys et al., 1999; Saenko et al., 2011) (**Figure 2S, Figure 3S, Figure 4O, Figure 5M, Figure 6N, Figure S3-S6**).

20) *engrailed* (*en*) was expressed in the posterior compartment and in the eyespot centers consistent with previous studies (Banerjee et al., 2020; Keys et al., 1999; Monteiro et al., 2006; Reed et al., 2020) (**Figure 2T, Figure 6O, Figure S3-S6**).

21) *Antennapedia* (*Antp*) was expressed in the eyespot centers consistent with previous studies (Oliver et al., 2012; Saenko et al., 2011; Shirai et al. 2012) (**Figure 2U, Figure 3T, Figure 4P, Figure 5N, Figure 6P, Figure S3-S6**).

22) *decapentaplegic (dpp)* was expressed along the AP boundary and lower posterior compartment consistent with a previous study (Banerjee and Monteiro, 2020a). *dpp* was also expressed in the intervein cells spanning the veins with missing expression in the eyespot centers during later stages (2.50-3.25), consistent with a previous study (Connahs et al., 2019a) (**Figure 2V, Figure 3U, Figure 4Q, Figure 5O, Figure 6Q, Figure S3-S6**).

23) *patched (ptc)* was expressed along the AP boundary, consistent with previous studies in butterflies (Banerjee and Monteiro, 2023; Keys et al., 1999; Saenko et al., 2011) and *Drosophila* (Phillips et al., 1990) (**Figure 2W, Figure 3V, Figure 4R, Figure 5P, Figure 6R, Figure S3-S6**).

24) *Mothers against dpp 6 (Mad6)* was expressed in two large clusters of cells along the AP domain and in the posterior compartment consistent with previous results (Banerjee and Monteiro, 2023) (**Figure 2X, Figure 3W, Figure 5Q, Figure S3-S6**).

25) *Notch* was expressed in the intervein cells during the earlier stages (0.75-1.00), and had a stronger expression in the eyespot centers during later stages (2.50), consistent with previous studies (Oliver et al., 2012; Reed and Serfas, 2004) (**Figure 3X, Figure 6S, Figure S3-S6**).

26) *spalt* was expressed in four distinct domains during the early larval stages (0.75-1.00), and in the eyespot center during the later stages (2.50-3.25), consistent with previous studies (Banerjee and Monteiro, 2020a; Matsuoka and Monteiro, 2022; Oliver et al., 2012; Wee et al., 2022) (**Figure 2Y, Figure 3Y, Figure 4S, Figure 5R, Figure 6T, Figure S3-S6**).

27) *Optix* was expressed in two distinct domains in the upper anterior and in the lower posterior compartment in the forewing and in the upper anterior compartment in the hindwing consistent with previous studies (Banerjee and Monteiro, 2020a; Banerjee and Monteiro, 2023) (**Figure 2Z, Figure 3Z, Figure 4T, Figure 5S, Figure 6U, Figure S3-S6**). *Optix* expression has been widely studied in the pupal wings of *Heliconius* butterflies (Reed et al., 2011).

28) *aristaless-like (al-like /al2)* was expressed in a band along the proximal axis consistent with a previous study in butterflies (Martin and Reed, 2010) (**Figure 2AA, Figure 3AA, Figure 5V, Figure S3-S6**).

29) *enhancer of split mbeta (ensl)* was newly visualized in provein cells adjacent to the veins, from early to late stages of wing development (**Figure 2AB, Figure 3AB, Figure 4U, Figure 5U, Figure S3-S6**).

30) *eyegone (eyg)* was newly visualized along the wing margin in intervein cells (**Figure 2AC, Figure 3AC, Figure 4V, Figure 5W, Figure S3-S6**).

31) *bric-a-bac (bab)* was newly visualized in larval wings expressed in distinct domains in the anterior compartment (**Figure 2AD, Figure 3AD, Figure 4W, Figure 6V, Figure S3-S6**). A previous study has looked at the expression of *bab* in pupal *Colias eurytheme* butterflies (Ficarrotta et al., 2022).

32) *nebula* (uncharacterized gene: XP_023941093.2) was a newly visualized gene expressed strongly along a proximal band, and at lower levels throughout the wing tissue (**Figure 2AE, Figure 3AE, Figure 4X, Figure S3-S6**).

33) *vestigial* (*vg*) was expressed in a broad domain along the wing margin consistent with a previous study in butterflies (Banerjee et al., 2023) and in *Drosophila* (Neumann and Cohen, 1997) (**Figure 2AF, Figure 3AF, Figure 5X, Figure 6W, Figure S3-S6**).

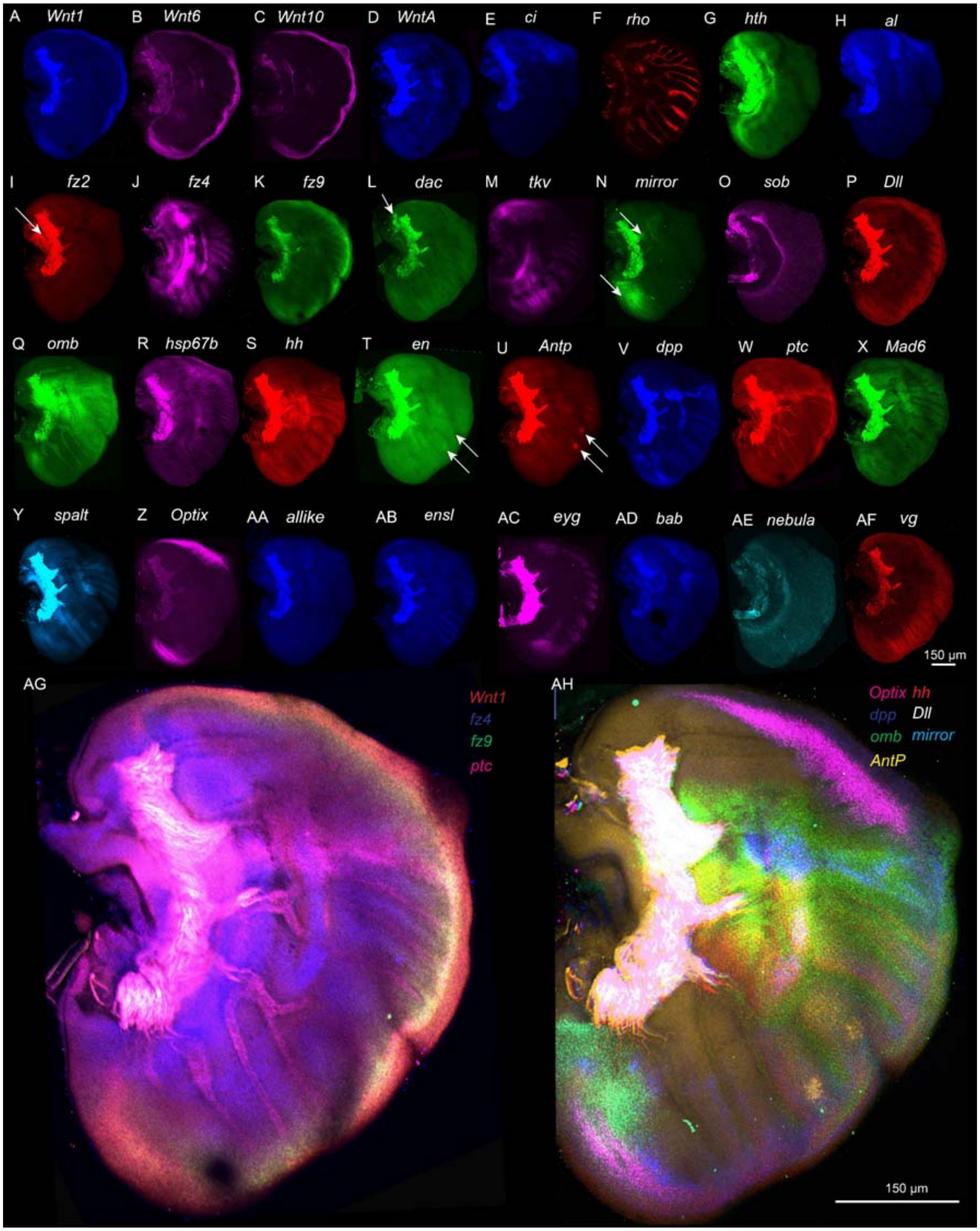
A Wnt1
B Wnt6
C Wnt10
D WntA
E ci
F rho
G hth
H al
I fz2
J fz4
K fz9
L dac
M tkv
N mirror
O sob
P Dll
Q omb
R hsp67b
S hh
T en
U Antp
V dpp
W ptc
X Mad6
Y spalt
Z Optix
AA allike
AB ensl
AC eyg
AD bab
AE nebula
AF vg
150 μm
AG
Wnt1
fz4
fz9
ptc
AH
Optix hh
dpp Dll
omb mirror
AntP
150 μm

Figure 2. Multiple genes are visualized in a single larval forewing of *Bicyclus anynana* (Stage 0.75). (**A-AF**) Expression of individual target genes (arrows indicate small expression domains); (**AG**) Co-expression of *Wnt1, fz4, fz9,* and *ptc*; (**AH**) Co-expression of *Optix, dpp, omb, Antp, hh, Dll,* and *mirror*. Experiment performed using manual multiplexing.

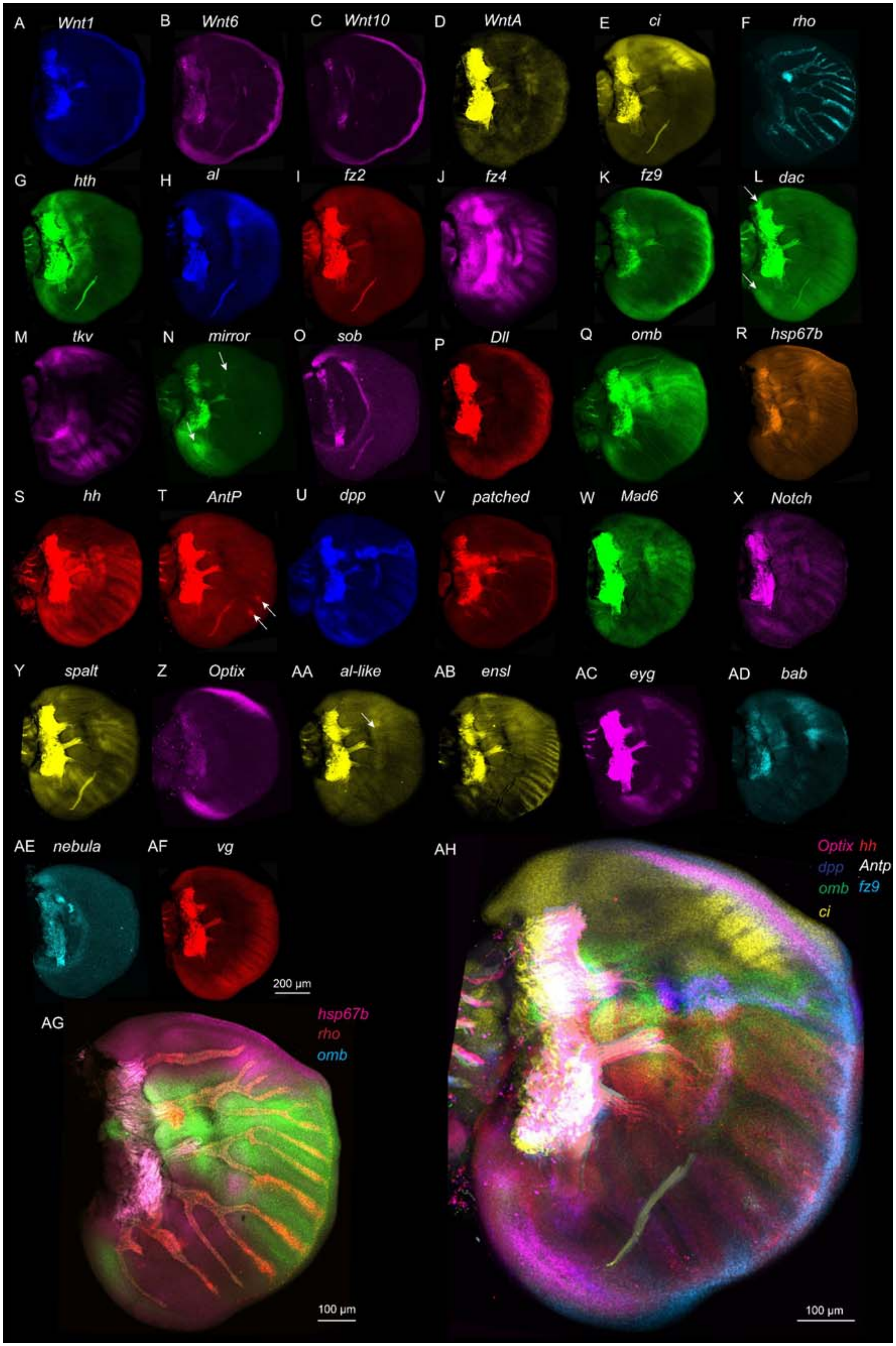
A Wnt1
B Wnt6
C Wnt10
D WntA
E ci
F rho
G hth
H al
I fz2
J fz4
K fz9
L dac
M tkv
N mirror
O sob
P Dll
Q omb
R hsp67b
S hh
T AntP
U dpp
V patched
W Mad6
X Notch
Y spalt
Z Optix
AA al-like
AB ensl
AC eyg
AD bab
AE nebula
AF vg
200 µm
AG
hsp67b
rho
omb
100 µm
AH
Optix hh
dpp Antp
omb fz9
ci
100 µm

Figure 3: Detection of 32 genes in an early larval forewing of *Bicyclus anynana* (stage 1.00). (**A-AF**) Expression of multiple target genes (arrows indicate small expression domains); (**AG**) Co-expression of *omb*, *rho*, and *hsp67b*; (**AH**) Co-expression of *Optix*, *dpp*, *omb*, *ci*, *hh*, *Antp*, and *fz9*. Experiment performed using manual multiplexing.

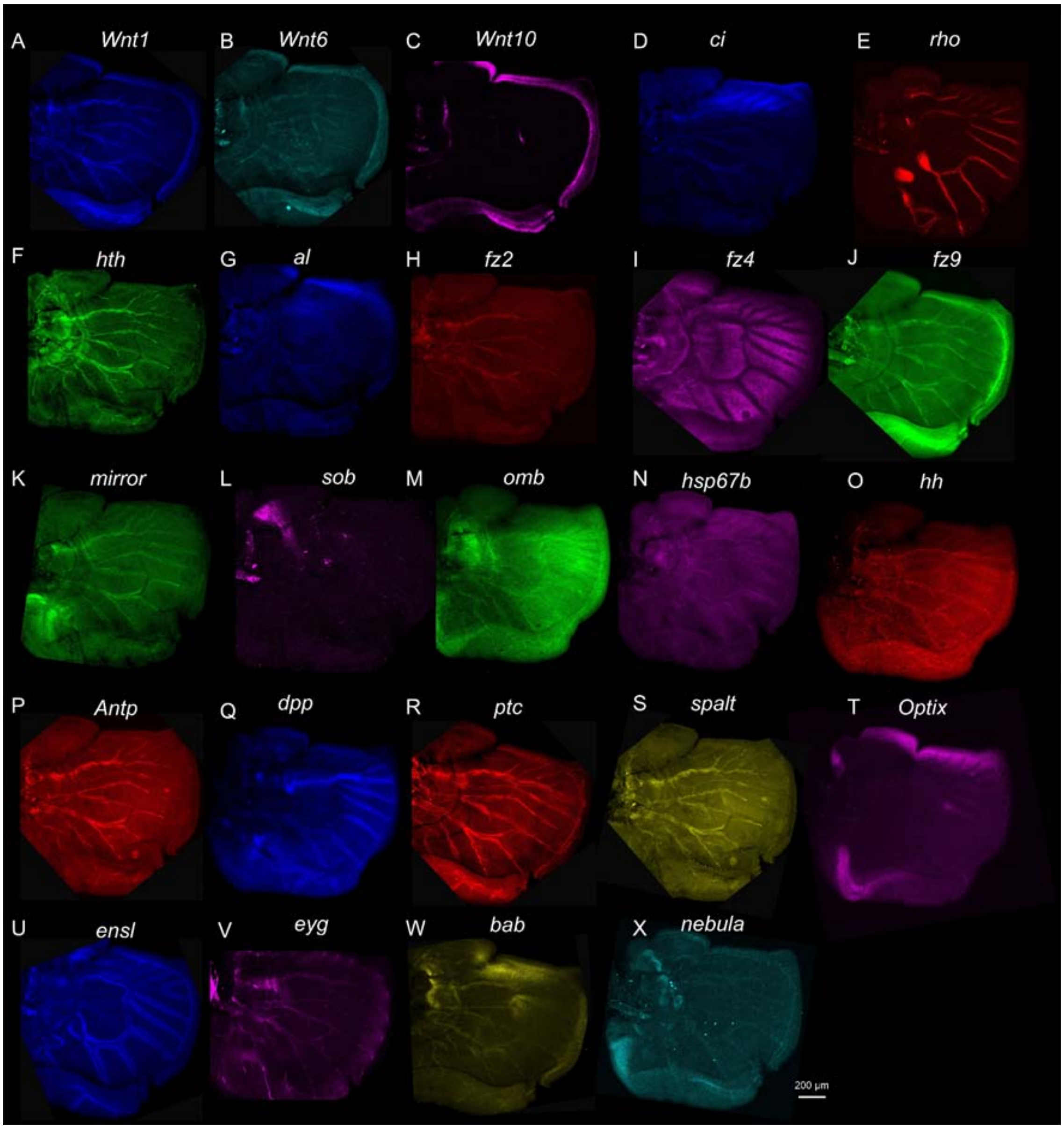
A Wnt1
B Wnt6
C Wnt10
D ci
E rho
F hth
G al
H fz2
I fz4
J fz9
K mirror
L sob
M omb
N hsp67b
O hh
P Antp
Q dpp
R ptc
S spalt
T Optix
U ensl
V eyg
W bab
X nebula
200 µm

Figure 4. Expression of 24 genes in a late larval forewing of *Bicyclus anynana* (stage 3.25). (**A-X**) Expression of multiple target genes. Experiment performed using manual multiplexing.

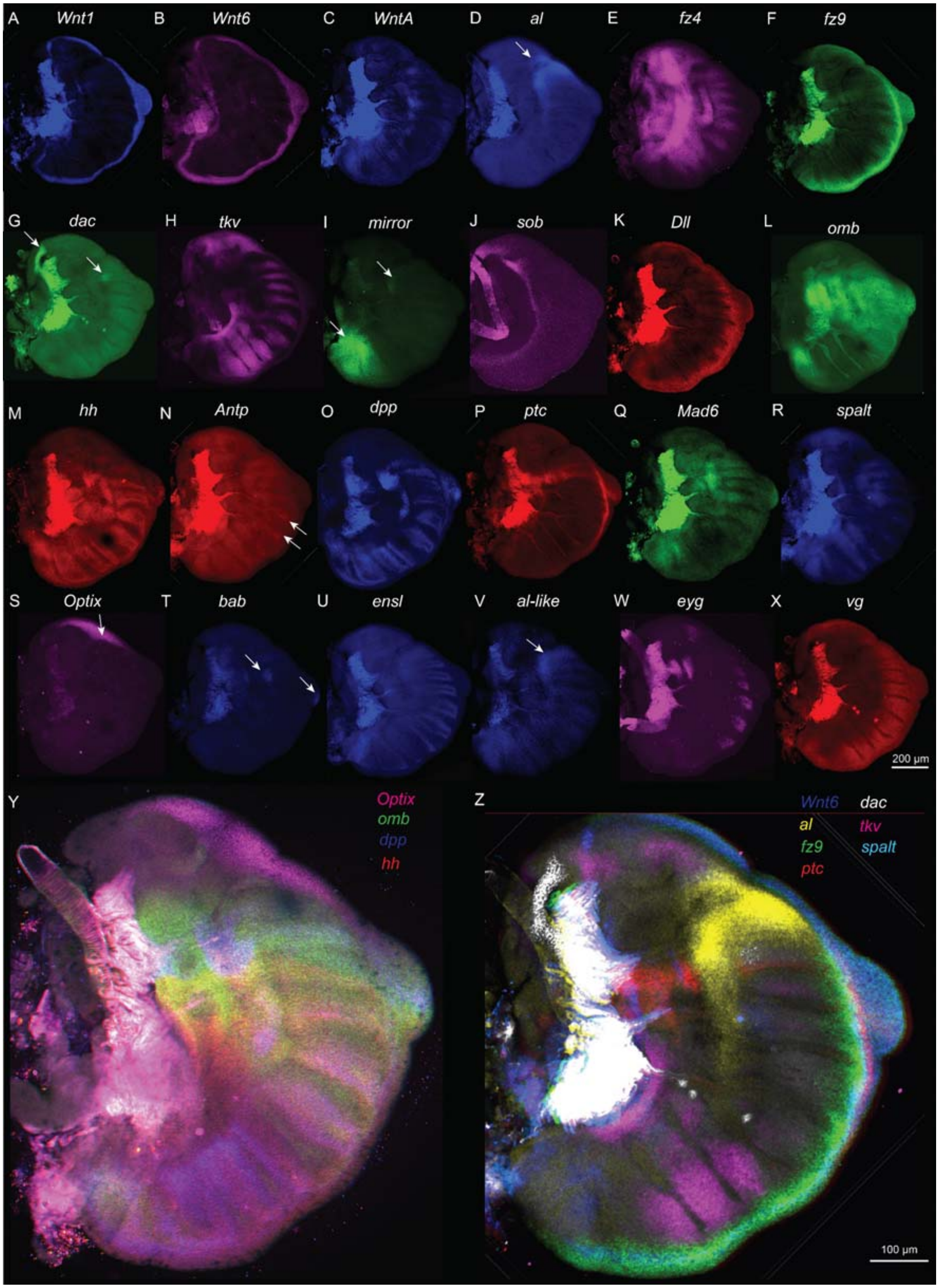
A Wnt1
B Wnt6
C WntA
D al
E fz4
F fz9
G dac
H tkv
I mirror
J sob
K Dll
L omb
M hh
N Antp
O dpp
P ptc
Q Mad6
R spalt
S Optix
T bab
U ensl
V al-like
W eyg
X vg
200 µm
Y
Optix
omb
dpp
hh
Z
Wnt6
dac
al
tkv
fz9
spalt
ptc
100 µm

Figure 5. Expression of 24 genes in a late larval hindwing of *Bicyclus anynana* (stage 1.00). (**A-X**) Expression of multiple target genes (arrows indicate small expression domains); (**Y**) Co-expression of *Optix*, *omb*, *dpp*, and *hh*; (**Z**) Co-expression of *Wnt6*, *al*, *fz9*, *ptc*, *dac*, *tkc*, and *spalt*. Experiment performed using manual multiplexing.

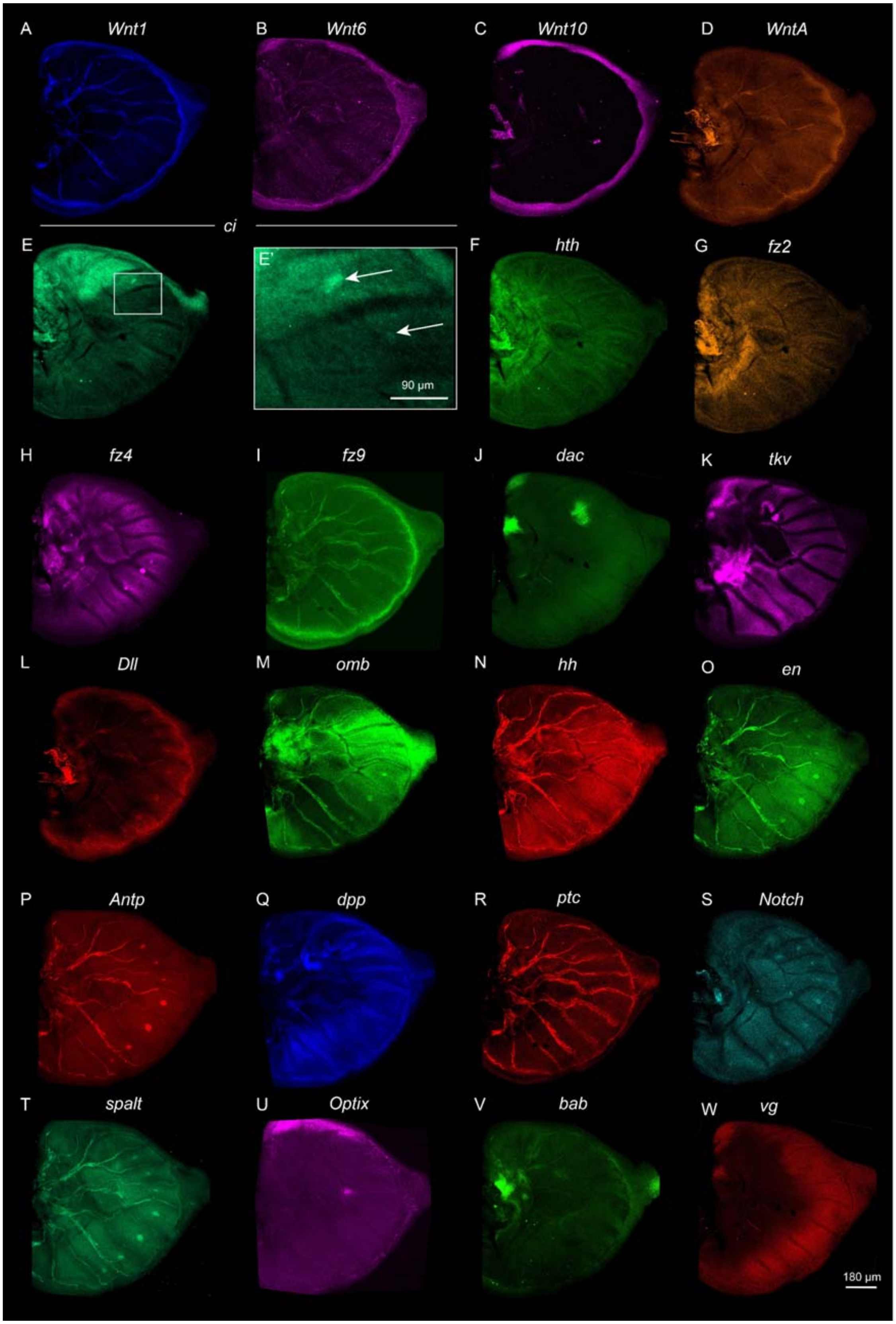
A
Wnt1
B
Wnt6
C
Wnt10
D
WntA
ci
E
E'
90 µm
F
hth
G
fz2
H
fz4
I
fz9
J
dac
K
tkv
L
Dll
M
omb
N
hh
O
en
P
Antp
Q
dpp
R
ptc
S
Notch
T
spalt
U
Optix
V
bab
W
vg
180 µm

Figure 6. Expression of 23 genes in a late larval hindwing of Bicyclus anynana (stage 2.50). (A-W) Expression of multiple target genes. **(E)** Expression of *ci* in the M1 and M2 eyespot centers (white arrows). Experiment performed using manual multiplexing.

Robustness analysis: Qualitative and quantitative measurement of signal quality after multiple cycles

We performed a robustness analysis to quantify the signal degradation due to multiplexing. To achieve this, we examined the expression of the gene *optomotor-blind* (*omb*) after multiple cycles, at cycle 1 and cycle 12. The aligned wings from the experiment were imported in FIJI **(Figure S7).** Colocalization plots between the two images were generated using the 'Colocalization finder' plugin **(Figure S7 C, G, and K).** Pearson coefficient (R) values were generated by selecting Analyse -> Colocalization -> Colocalization test. To calculate the area of expression, color thresholding with a brightness filter of 100 was applied. The selected regions were measured and imported into an Excel sheet to generate the graphs **(Figure S7D, H, and L).** We confirmed that *omb* expression was qualitatively similar between cycles with clear expression domains spanning Anterior-Posterior boundary and in the eyespot centers as expected **(Figure S7 A, B, E, F, I, and J).** Some quantitative reduction due to degradation of RNA levels were observable in the samples **(Figure S7 D, H, and L)**.

Automated multiplexing in *Danio rerio* larvae

Danio rerio have remained a popular model organism for behavioral studies and neurobiology (Gerlai, 2020). Larval *Danio rerio*, particularly pigment free mutants (Antinucci and Hindges, 2016), are ideal for high throughput spatial gene expression techniques because they are abundant, transparent, require no special preparation before the procedure, and are small enough to process dozens of animals in parallel. Spatial transcriptomic profiles add unique insights on the brain functionality and circuit level connections between brain regions that bulk and single cell RNA sequencing alone cannot reveal. One way in which this was achieved recently was by registering *in situ* results from individual staining to a standard reference brain (Schulze et al., 2023). However, these existing datasets focus on young larvae (< 6 dpf). Maps of gene expression in late-stage larvae or juvenile fish brains when complex behaviors including learning and social behaviors emerge are limited or absent (Gemmer et al., 2022). We performed the multiplexing experiment using the automation system on 10 and 14 days post fertilization (dpf) larvae to examine gene expression in the brain (**Figure 7**). Here, we spatially profiled six genes to illustrate the use of RAM-FISH. We examined receptor genes that have low expression levels (such as *chrna5*), neurotransmission associated genes that have broad brain-wide expression (such as *neurod1* and *gad2*), and neuropeptide genes, that are expressed in a few neurons in deep seated brain regions (such as *oxt* expressing neurons in hypothalamus). Overall, the expression patterns observed are consistent with previous reports available at mapzebrain (https://mapzebrain.org/home), or Zebrafish Information Network (ZFIN; **Table S2**) for younger larvae. The expression of the following genes was observed.

1) *glutamate decarboxylase 2 (gad2)* was expressed widely throughout the brain with strong expression in sub-pallial regions, preoptic area, as well as cerebellar regions (Filippi et al., 2014). (**Figure 7A and H, Figure S9A**).

2) *olfactory marker protein b (omp)* was expressed in the olfactory receptor neurons in the anterior forebrain expression. In addition, faint expression was present in a few neurons in the telencephalon (forebrain) around the eyes (Çelik et al., 2002). (**Figure 7B, Figure S9B**).

3) *nicotinic acetylcholine receptor subunit alpha 5* (*chrna5)* was expressed in the dorsal habenula with faint expression in the olfactory bulb, tectum and along the periphery of medula oblangata (Mueller and Wullimann, 2002) (**Figure 7C, Figure S9C**).

4) *neuropilin 1a (nrp1a)* was asymmetrically expressed in the left dorsal habenula and sparsely in the diencephalic or the midbrain neurons (Kuan et al., 2007) (**Figure 7D and H, Figure S9D**).

5) *neuronal differentiation 1 (neuroD)* expression was widespread throughout the brain, including cerebellum, diencephalon and telencephalon (Mueller and Wullimann, 2002) (**Figure 7E and H, Figure S9E**).

6) *oxytocin (oxt*) was expressed symmetrically in the anterior hypothalamus, in a restricted cluster of cells (Unger and Glasgow, 2003) (**Figure 7F, Figure S9F**).

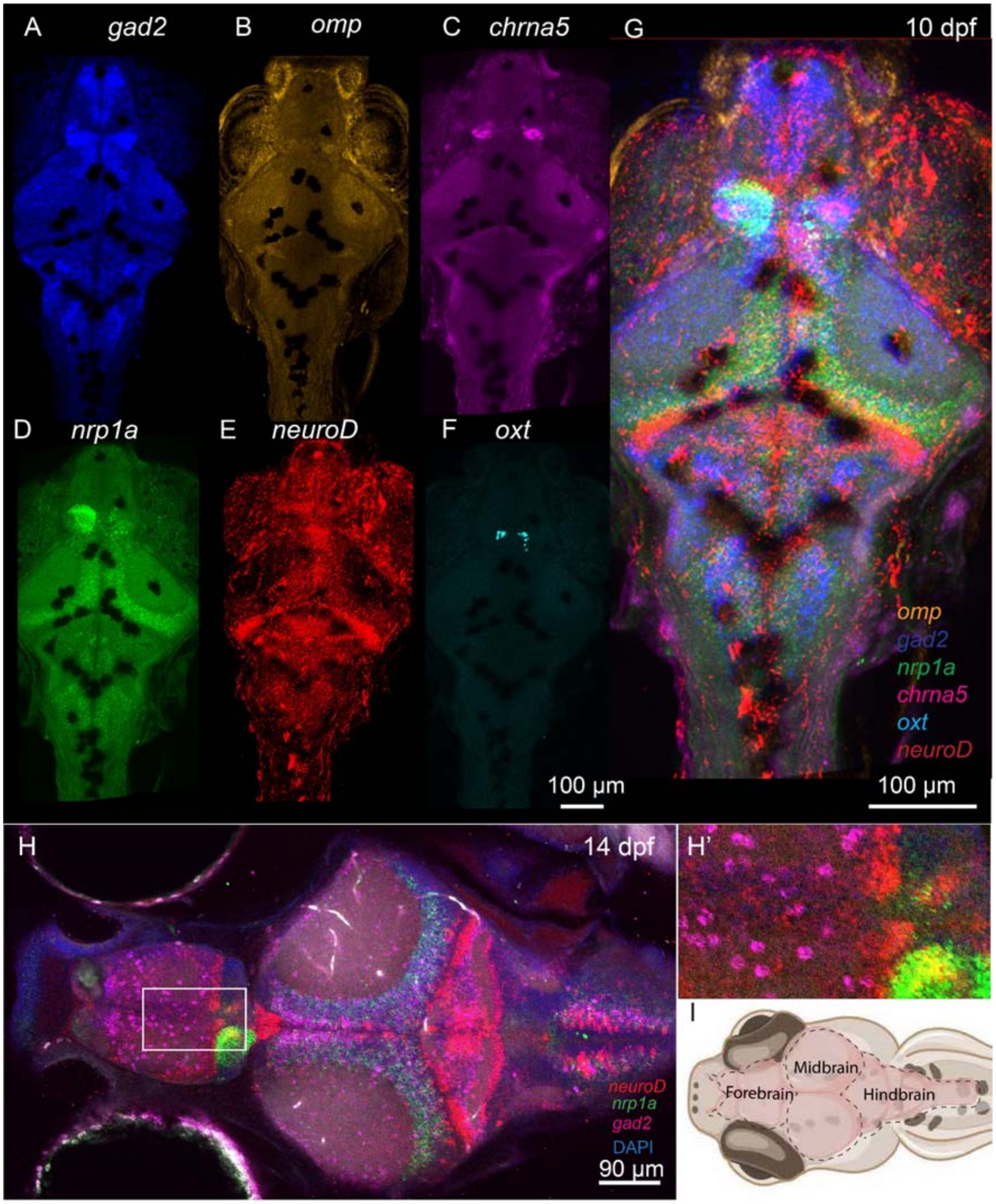
A gad2
B omp
C chrna5
G
10 dpf
D nrp1a
E neuroD
F oxt
omp
gad2
nrp1a
chrna5
oxt
neuroD
100 µm
100 µm
H
14 dpf
H'
neuroD
nrp1a
gad2
DAPI
90 µm
I
Midbrain
Forebrain
Hindbrain

Figure 7. Detection of multiple gene targets in 10 and 14 dpf *Danio rerio* larvae. (A-F) Multiplexed detection of target genes in 10 dpf *Danio rerio* larva. **(G)** Merged, z-stacked image of *omp*, *gad2*, *nrp1a*, *chrna5*, *oxt* and *neuroD* multiplexed expression. (**H**) Merged image of *gad2*, *nrp1a*, and *neuroD* in a single z-section of a 14 dpf *Danio rerio* larva. (**H'**) Inset of H (white rectangle) at higher resolution displaying cellular localization in the forebrain. (**I**) Schematic of the anatomy of the larval brain. Experiments were performed using automated multiplexing.

Discussion

Spatial RNA profiling technologies, which involve quantification and localization of RNA transcripts, are rapidly evolving and are capable of profiling thousands of mRNA species. The technologies are accelerating basic and applied research, including in the fields embryology and organ development (Choi et al., 2023; Rao et al., 2021; Zhang et al., 2021), neurobiology (Jung and Kim, 2023; Moffitt et al., 2018), and cancer research (Coutant et al., 2023; De Zuani et al., 2024; Valdeolivas et al., 2024; Wu et al., 2021a; Wu et al., 2021b; Wu et al., 2023; Zhang et al., 2022; Zhou et al., 2023b). Yet they face major limitations such as 1) complex and costly setups for dedicated sequencing, microfluidics, and imaging; 2) extensive time consuming steps to perform each experiment; 3) complex analyses pipelines; 4) special sample preparations which are often limited to 2D sections of 7-10 µm; and 5) mRNA detection errors.

Our goal was to solve these limitations by deploying a cost effective, less complex, and faster spatial profiling methodology that can be adapted quickly by laboratories. To achieve this, we modified previously described methods. We modified the widely used HCR3.0 amplification reaction (Choi et al., 2018) by deploying thermal control inside the reaction chamber and by modifying the buffers. We used a DNase I based signal removal strategy (Codeluppi et al., 2018; Kishi et al., 2019; Shah et al., 2016; Sternson et al., 2022; Wang et al., 2021), followed by reprobing and imaging, to achieve multiplexing. Finally, the methodology is not restricted to thin slices of tissue, allowing multiplexing experiments on intact organs and animals. As demonstrated here for butterfly wings and whole fish larvae, this methodology can be applied to diverse species with or without automation.

It will be of most use to developmental biologists, developmental geneticists and pathologists, who often only need high quality spatial information on dozens of genes, with or without absolute quantification of mRNA levels in the tissues. This technology will aid in basic studies of pattern formation, embryological development, and in dissecting the architecture of gene-regulatory networks. For instance, the multiplexed *in-situ* images, when combined with functional tools such as CRISPR-Cas9, drug inhibitors, and RNAi, can be used to test how perturbations to single genes affect the expression of multiple possible targets. The current method can also complement other technologies such as single-cell and laser-based spatial transcriptomics (Banerjee et al., 2022; Datta et al., 2015; Liu et al., 2019; Nichterwitz et al., 2016; Nichterwitz et al., 2020; Saliba et al., 2014; Shalek et al., 2014).

In the present work, we provided atlases of multiple known and newly visualized genes during different stages of larval wing development of *Bicyclus anynana* butterflies (~80-100 µm thick), as well as larval fish brains, which can be used as references in future research. Many classic genes such as *WntA*, *Optix*, *spalt*, *dpp*, *Dll*, *Antp*, *vg*, *hh*, *notch*, and *ptc*; and newly visualized genes such *hth*, *dac*, *hsp67b*, *nebula*, *bab*, and *eyg*, showed highly consistent expression patterns in the multiple wing samples tested, supporting the reliability of the current methodology. We hope these results will inspire researchers to test the method in their own system.

Materials

HCR3.0 Buffers (from Choi et al., 2018; Bruce et al., 2021)

All the chemicals unless mentioned were ordered from Sigma-Aldrich (Merck).

30% probe hybridization buffer:

Composition: 30% formamide (Cat No. F7503-1L), 5× sodium chloride sodium citrate (SSC), 9 mM citric acid (Cat No. 251275-100G) (pH 6.0), 0.1% Tween 20 (Cat No. P1379-100ML), 50 µg/mL heparin (Cat No. H3393-50KU), 1× Denhardt's solution (Cat No. D2532-5X5ML), and 5% dextran sulfate (Cat No. D6001-50G).

For 40 mL of solution:

Mix in a 50 ml conical tube (Cat No. BS-500-MJL-S) 12 mL formamide (Cat No. F7503-1L), 10 mL of 20× SSC, 360 µL 1 M citric acid (Cat No. 251275-100G), pH 6.0, 40 µL of Tween 20 (Cat No. P1379-100ML), 200 µL of 10 mg/mL heparin (Cat No. H3393-50KU), 800 µL of 50× Denhardt's solution (Cat No. D2532-5X5ML), and 4 mL of 50% dextran sulfate (Cat No. D6001-50G). Fill up to 40 mL with DEPC (Cat No. D5758-25ML) H_2O.

30% probe wash buffer

Composition: 30% formamide (Cat No. F7503-1L), 5× sodium chloride sodium citrate (SSC), 9 mM citric acid (Cat No. 251275-100G) (pH 6.0), 0.1% Tween 20 (Cat No. P1379-100ML), and 50 µg/mL heparin (Cat No. H3393-50KU).

For 40 mL of solution

Mix in a 50 ml tube 12 mL formamide (Cat No. F7503-1L), 10 mL of 20× SSC, 360 µL 1 M citric acid (Cat No. 251275-100G), pH 6.0, 40 µL of Tween 20 (Cat No. P1379-100ML), and 200 µL of 10 mg/mL heparin (Cat No. H3393-50KU). Fill up to 40 mL with DEPC H_2O.

50% dextran sulfate

For 40 mL of solution

Mix in a 50 ml tube 20 g of dextran sulfate powder (Cat No. D6001-50G). Fill up to 40 mL with DEPC H_2O.

Amplification buffer

5× sodium chloride sodium citrate (SSC), 0.1% Tween20, and 5% dextran sulfate (Cat No. D6001-50G).

For 40 mL of solution

Mix in a 50 ml tube 10 mL of 20× SSC, 40 µL of Tween 20 (Cat No. P1379-100ML), 4 mL of 50% dextran sulfate (Cat No. D6001-50G). Fill up to 40 mL with DEPC H_2O.

Detergent Solution

Composition: 1.0% SDS (Cat No. 436143-25G), 2.5% Tween (Cat No. P1379-100ML), Tris-HCl (Cat No. 10812846001) (pH 7.5), 1.0 mM EDTA (Cat No. E9884-100G) (pH 8.0), and 150.0 mM NaCl (Cat No. S9888-25G).

For 50 mL of Solution

Mix in a 50 ml tube 5.00 mL 10% SDS (Cat No. 436143-25G) (filtered), 1.25 mL Tween 20 (Cat No. P1379-100ML), 2.50 mL 1M Tris-HCl (Cat No. 10812846001), pH 7.5, 0.10 mL 0.5 M EDTA (Cat No. E9884-100G), pH 8.0, 1.50 mL 5 M NaCl (Cat No. S9888-25G). Fill up to 50 mL with DEPC H_2O.

1x PBST (for 50 ml of solution)

5ml 10x PBS, 50 µL Tween 20 (Cat No. P1379-100ML). Fill up to 50mL with water.

5× SSCT (for 40 mL of solution)

10 mL of 20× SSC, 40 µL of Tween 20 (Cat No. P1379-100ML). Fill up to 40 mL with DEPC H_2O.

DEPC H_2O (1000 ml)

Add 1ml of DEPC to 1000 ml of MilliQ water. Mix well and store in dark overnight. The next day autoclave.

10x PBS

For 1 liter of solution add 81.8 g of NaCl (Cat No. S9888-25G), 5.28g of KH_2PO_4, (Cat No. P0662-25G) and 10.68 g of K_2HPO_4. (Cat No. P3786-100G) in a glass bottle. Fill till 1000ml using dH_2O and autoclave. Store at RT for up to 6 months.

20x SSC

For 1000 ml of solution add 175.3 g of NaCl (Cat No. S9888-25G) and 88.2 g of trisodium citrate (Cat No. S1804-500G). Add dH_2O till 1000 ml and autoclave. Store at RT for up to 6 months.

List of modified buffers used in the automation system/manual methodology

Hybridization buffer

20% EC hybridization buffer:

Composition: 20% ethylene carbonate (Cat No. E26258-3KG), 5× sodium chloride sodium citrate (SSC), 12 mM citric acid (pH 6.0) (Cat No. 251275-100G), 0.5% Tween 20 (Cat No. P1379-100ML), 100 µg/mL heparin (Cat No. H3393-50KU), 1.2× Denhardt's solution (Cat No. D6001-50G), 2.5% dextran sulfate (Cat No. D6001-50G), 1.0mM EDTA (pH 8.0) (Cat No. E9884-100G).

For 50 mL of solution:

Mix in a 50 ml tube 10 mL ethylene carbonate (Cat No. E26258-3KG), 12 mL of 20× SSC, 400 µL 1 M citric acid (pH 6.0 (Cat No. 251275-100G), 200 µL of Tween 20 (Cat No. P1379-100ML), 400 µL of 10 mg/mL heparin (Cat No. H3393-50KU), 1000 µL of 50× Denhardt's solution (Cat No. D6001-50G), 5 mL of 25% dextran sulfate (Cat No. D6001-50G), 100 µl of 500mM EDTA (pH8.0) (Cat No. E9884-100G). Fill up to 50 mL with DEPC (Cat No. D5758-25ML) H_2O.

Wash buffer

20% EC wash buffer:

Composition: 20% ethylene carbonate (Cat No. E26258-3KG), 5× sodium chloride sodium citrate (SSC), 12 mM citric acid (pH 6.0) (Cat No., 0.5% Tween 20 (Cat No. P1379-100ML), and 100 µg/mL heparin (Cat No. H3393-50KU).

For 50 mL of EC wash solution:

Mix in a 50 ml tube 10 mL ethylene carbonate (Cat No. E26258-3KG), 10 mL of 20× SSC, 400 µL 1 M citric acid (Cat No.), pH 6.0, 200 µL of Tween 20 (Cat No. P1379-100ML), 400 µL of 10 mg/mL heparin (Cat No. H3393-50KU). Fill up to 50 mL with DEPC (Cat No.) H_2O.

Note: The use of ethylene carbonate accelerates the overall FISH hybridization time. Previous reports have suggested use of 15-20% ethylene carbonate as an alternative accelerates DNA-FISH experiments (Kalinka et al., 2020; Matthiesen and Hansen, 2012). 10% ethylene carbonate has also been used in hybridization mixture and wash buffer in MERFISH experiments (Fang et al., 2023; Moffitt et al., 2016a). The buffer presented in this study will freeze in 4°C. Kindly thaw before starting the experiment or prepare fresh.

Imaging Buffer:

Composition: 70% glycerol (Cat No. G7893-500ML) with 1.0mM EDTA (pH 8.0) (Cat No. E9884-100G). For 50 ml solution in a 50ml tube add 35ml 100% glycerol and 100 µl of 500 mM EDTA. Top up to 50 ml using DEPC water, adjust the pH to 7.8, and store at room temperature for up to 2 months.

Alternative, use 2mM Trolox (Cat No. 238813-5G), 10% w/v glucose (Cat No. G7021-100G), 0.1mg/ml glucose oxidase (Cat No. 345386-10KU), 50 ug/ml catalase (Cat No. C9322-5G), 5x SSC, Tris-HCl (Cat No. 10812846001) 50mM. If possible, prepare fresh, else use within 1 week.

Permeabilization Solution:

Composition: 4.0% Ammonium lauryl sulfate (Cat No. 09887-250ML), 5.0% Tween 20 (Cat No. P1379-100ML), Tris-HCl pH 7.5 (Cat No. 10812846001), 1.0 mM EDTA pH 8.0 (Cat No. E9884-100G), and 200.0 mM NaCl (Cat No. S9888-25G).

For 50 mL of Solution:

Mix in a 50 ml tube 10.00 mL 20% Ammonium lauryl sulfate (Cat No. 09887-250ML) (filtered), 2.50 mL Tween 20 (Cat No. P1379-100ML), 2.50 mL 1M Tris-HCl (Cat No. 10812846001), pH 7.5, 0.10 mL 0.5 M EDTA (Cat No. E9884-100G) pH 8.0, and 2.00 mL 5 M NaCl (Cat No. S9888-25G). Fill up to 50 mL with DEPC H_2O.

Note: The use of ammonium lauryl sulfate provides an alternative to the harsh sodium dodecyl sulfate (SDS) for permeabilization of the probes. Store at RT or 4°C for up to 2 months.

Mounting Media:

Composition: 70% glycerol (Cat No. G7893-500ML) with 1.0mM EDTA (pH 8.0) (Cat No. E9884-100G). For 50 ml solution in a 50 ml tube add 35ml 100% glycerol and 100 µl of 500 mM EDTA. Top up to 50 ml using DEPC water, adjust the pH to 7.8, and store at room temperature for up to 2 months.

Alternatively prepare, 2 mM Trolox (Cat No. 238813-5G), 10% w/v glucose (Cat No. G7021-100G), 0.1mg/ml glucose oxidase (Cat No. 345386-10KU), 50 ug/ml catalase (Cat No. C9322-5G), 5x SSC, Tris-HCl (Cat No. 10812846001), 50mM, 60% Glycerol (Cat No. G5516-100ML). Modified from ref (Zhang et al., 2021). If possible, prepare fresh. Else, store at 4°C and use within 1-2 weeks after preparation.

DAPI buffer:

For 1ml of solution add 5 µl of stock DAPI (Cat No. D9542-5MG) (1mg/ml in DMSO) in 995 µl of 5x SSCT in a 1.5ml tube. Prepare fresh before use.

Signal removal and wash solutions

Signal removal solution (1ml): In a 1.5 ml tube add Tris pH7.5 (Cat No. 10812846001 (1M) – 100 µl, $MgCl_2$ (Cat No. M8266-100G) (0.5M) – 50 µl, $CaCl_2$ (Cat No. C4901-100G) (0.5M) – 5 µl, DnaseI (ThermoFisher-Cat No.: EN0521) – 15 µl. Add dH_20 to fill till 1ml. Prepare fresh.

Note: Signal removal solution can remove the signal when kept at 37°C in 30-60 mins when performed manually and as fast as 15 mins in the robotic system in samples up to 50-100 µm thick.

Signal wash buffer 1 (10ml): In a 15 ml tube add Tris pH7.5 (Cat No. 10812846001) (1M) – 1000 µl, $MgCl_2$ (Cat No. M8266-100G) (0.5M) – 500 µl, $CaCl_2$ (Cat No. C4901-100G) (0.5M) – 50 µl. Add dH_20 to fill till 10ml.

Signal wash buffer 2 (1ml): In a 1.5 ml tube add Tris pH7.5 (Cat No. 10812846001 (1M) – 100 µl, $MgCl_2$ (Cat No. M8266-100G) (0.5M) – 50 µl, $CaCl_2$ (Cat No. C4901-100G)(0.5M) – 5 µl, 500mM EDTA pH 8.0 (Cat No. E9884-100G) – 5 µl, 10% SDS (Cat No L3771-100G) - 150 µl. Add dH_20 to fill till 1ml.

Note: Prepare the signal removal and wash buffers fresh.

Robot cleaning solution (20 ml)

Composition: 2% SDS (Cat No. 436143-25G), 1% Sodium dichloroisocyanurate (Cat No. 218928-25G) and 1% NaOH (Cat No. 221465-25G).

Alternatively, prepare 20ml of solution by mixing 5ml RNaseZap (ThermoFisher, Cat No. AM9780) and 15ml DEPC water.

Sample embedding in confocal dish:

Confocal dish (3.5 mm with glass cover slip) (SPL, Cat No. 101350): The attached glass coverslips are silanized based on the protocol described in (Moffitt et al., 2016b). Afterwards, 500ul of 0.01% poly-l-lysine (Cat No. P4707-50ML) is added on the glass surface of the confocal dish.

Fixed and permeabilized tissues are added and embedded in an acrylamide gel (see gel composition below). A gel free methodology is also described in the procedure section below.

Gel matrix:

Gel matrix composition

A polyacrylamide gel (**Table 1**) is necessary to keep thick tissues in place during the multiple rounds of hybridization, washing, imaging, and alignment. The gel will expand after buffers are added so it is important to cast a gel that is narrower than the 3.5 cm confocal dish. The expansion factor, i.e., the diameter of the gel (Dgel) by diameter of coverslips (Dcp) for different buffers is provided in Fang et al. (2023).

Table 1. Composition of polyacrylamide gel.

S.N.	Reagent	Volume/Weight
1.	DEPC H_2O	1080 µl
2.	NaCl (1M) (Cat No. S9888-25G)	600 µl
3.	Acrylamide (Cat No. A9099-100G)	160 mg
4.	Tris-HCl 1M (Cat No. 10812846001)	120 µl

5.	TEMED (Cat No. T9281-25ML)	10 µl
6	Ammonium persulfate (1% w/v) (Cat No. 248614-100G)	30 µl (prepared fresh every time)

Note: A smaller volume can be prepared based on user requirements.

Around 100 µl of the above solution was added on top of a narrowed confocal dish along with a circular coverslip on top (18mm diameter), pressed gently with a 3D printed solid cylinder (18mm Diameter, ~20 gms), and allowed to solidify. The solid cylinder and the coverslip were removed afterwards, and the confocal dish was either transferred to the arc chamber with a microcomb chip holder on top (**Figure 1E and F**) or for manual experimentation. Alternatively, cast the gel with sample on a glass slide with a coverslip on top and move the gel to the confocal dish.

Note: For clearing, the tissue can be left in the gel in 2% SDS, 0.5% Triton-X 100 in 2x SSC at 37°C overnight (Liu et al., 2022).

Procedure

Manual multiplexing protocol

A) Probe preparation

Preparing the primary stock solution (10 pairs of probes: 5µM final volume)

Up to 10 pairs of oligonucleotides were used, each at a concentration of 100 µM. 100 µl of oligos from each tube were mixed to form a master mix with a final probe concentration of 5 µM in a 2 ml microcentrifuge tube (Labselect, Cat No. MCT-001-200). Three to four genes with different hairpin amplifiers (Molecular Instruments) can be designed and tested in a single round of HCR. The number of genes tested in each round depends on the number of laser lines in the confocal being used. The stock mix of primary probes are stored at -20°C.

Prepare the 30% probe hybridization buffer or 20% EC hybridization buffer with probes complementary to the target RNA.

Preparation of DNA oligo mix: Add 10 µl of each of the 5 µM DNA oligo mixes for each gene (e.g., add 10+10+10 µl for 3 genes) in a 1.5 ml tube and adjust the volume to 1000 µl in 30% probe hybridization buffer or 20% EC hybridization buffer in a 1.5ml microcentrifuge tube (Labselect, Cat No. MCT-001-150).

Note: If you are targeting a lowly expressed gene you might need to either increase the concentration of the probes for that gene, or the number of probe pairs, in the DNA oligo mix.

Prepare the secondary probes with fluorescent tags.

Add 5 µl of each H1 and H2 hairpins (Molecular Instruments) separately in 150+150 µl of Amplification buffer in two 200 µl PCR tubes.

Heat at 95°C for 90 secs in a thermocycler and cool down at room temperature in a dark environment for 30 mins. Mix the two tubes together in a 1.5 ml microcentrifuge tube (Labselect, Cat No. MCT-001-150) and use.

Note: We use the following combinations: 1) B1: AF546, 2) B2: AF647, 3) B3: AF 488. We have used B4 with a AF514 tag which sometimes cross-talks with the AF546 fluorophores.

The secondaries can be used multiple times. After using the probes, collect them from the sample and store at -20°C. For repeated use, heat the secondary probes in dark in amplification buffer at 37-42°C for 30 mins before use.

A control protein marker, nuclear marker, or cell membrane marker is recommended for tracking the cells during different cycles of hybridization and imaging. DAPI signal from each round of hybridization can be used for cell registration (Sternson et al., 2022). Currently we are developing a protein marker based staining methodology with antibodies against a cell membrane marker in butterfly wings such as Armadillo (Banerjee and Monteiro, 2023) tagged with a secondary antibody (AF405; Invitrogen: Catalog # A48261). In the current work *Bicyclus anynana* wings from different FISH rounds were aligned in photoshop layers by aligning the wing margin boundaries and the auto fluorescent signal observed along the tracheal tissue. The *Danio rerio* larvae from different rounds were aligned using the melanin pigmentation marks.

For merging of up to 7 channels, the open source platform FIJI (Schindelin et al., 2012) was used. For creating a merged image, the aligned image files (with the same width and height) were imported in FIJI. Afterwards, Image -> Color -> Merge Channels was selected. C1 to C7 options from the drop-down menu with the specific file names were selected (make sure the 'create composite' box is selected). Then, 'OK' was selected to create the composite image.

B) Steps

Day 1

1) Dissect the tissue in 1x PBS at Room Temperature (RT ~ 22°C). For dissection of butterfly larval wings follow the protocol described in Banerjee and Monteiro, 2020b.

2) Transfer the tissue to either a 1.5ml tube or glass spot plate containing 500ul 1x PBST supplemented with 4% formaldehyde and fix for 30-60 mins at room temperature (RT) with shaking. Smaller fixation time is required for thinner tissues while longer time is required for thicker tissues.

4) Wash the tissue 3 times with 500 µl 1x PBST (3mins each) at RT.

5) Add 500 µl of detergent solution or alternative permeabilization solution (for more fragile samples) and leave the tissue for 30 mins at 37°C.

Note: If clearing tissue (for transparency) the tissue can also be left in 500ul of 10% SDS (Cat No. L3771-100G) + 2% boric acid (Cat No. B0394-100G) at 37°C for clearing for up to 10 hrs.

6) Wash 3 times with 500 µl 1x PBST (3 mins each) at RT.

7) Wash 2 times with 500 µl 5x SSCT (3 mins each) at RT.

Note: At this step you can either embed the sample in the acrylamide gel mentioned above or perform the experiment with the tissue free-floating in the buffer. For the free-floating experiments the reactions are carried out on glass spot plates (PYREX^{TM}; Corning, Corning, NY, USA; Cat. No.: 722085) or in 1.5 ml microcentrifuge tubes (Labselect, Cat No. MCT-001-150).

8) Transfer the tissues to 500 µl 30% probe hybridization buffer or 20% EC hybridization buffer and incubate at 37°C for 30 mins.

Note (Pause step): You can store the tissue in 30% probe hybridization buffer at 4°C for over 2 weeks without any significant reduction in signal quality. Do not store samples in the 20% EC hybridization buffer as the solution will crystallize at 4°C.

9) Prepare 1000 µl 30% probe hybridization buffer or 20% EC hybridization buffer supplemented with DNA oligos complementary to the target RNA (**described above**).

10) Remove the 30% probe hybridization buffer or 20% EC hybridization buffer added before and replace it with 500µl of the solution mentioned in step 9 supplemented with DNA oligos at 37°C.

12) Incubate the samples at 37-40°C for 8-16 hrs.

Note: Lower temperature (~30°C) might be necessary for certain probes for efficient binding.

Day 2

13) Incubate the samples in 30% probe wash buffer or 20% EC wash buffer stock solution at 37°C for 30 mins before washing.

14) Wash 4 times with 500 µl of 30% probe wash buffer/20% EC wash buffer (15 mins each).

15) Take out the plate from the 37°C incubator.

16) Wash 2 times with 500 µl 5x SSCT (3 mins each) at RT.

17) Incubate the tissue in 500 µl Amplification buffer for 30 mins at RT.

12) Replace the Amplification buffer with 200ul secondary probes (**described above**) at RT.

Note: It is critical to keep the sample away from light as much as possible from this step onwards.

13) Incubate the samples in the dark for 4-10 hrs at RT or 37°C.

14) Wash the tissue 5 times with 500 µl 5x SSCT (in a dark environment) for 10 mins each at 37°C.

Note: If you want to stain nuclei add 5 µL of DAPI to 500 µL 5x SSCT and incubate for 5 mins. Afterwards wash 2 times with 500 µL 5x SSCT for 3 mins each. You can leave the tissue in 5x SSCT overnight.

15) Replace the 5x SSCT with fluorescent mounting buffer or media and proceed for confocal imaging.

Note: If you are performing the experiment with free floating tissue in buffer, mount the sample on a slide, add mounting media, place coverslip, and proceed for imaging. Do not seal the coverslip. After imaging, remove the coverslip and wash with 5x SSCT to remove the sample from the glass slide. For experiments on microtome sectioned tissues (10-50 µm sections) on coverslips all the reactions and washes can be directly performed on the coverslips.

If you are performing the experiment in the acrylamide gel add imaging buffer and proceed for imaging.

16) For the second round of hybridization with a new set of probes, you need to remove the first set of probes. To remove the signal, first wash the tissue two times with 500 µl 5xSSCT at RT.

17) Wash 3 times with 500 µl signal wash buffer 1 at 37°C for 3 mins each.

18) Add 500 µl of signal removal solution and incubate at 37°C for 15-90mins (depending on the thickness of the tissue).

19) Wash 2 times with 500 µl signal wash buffer 2 at 37°C for 2 mins each.

20) Wash 3 times with 500 µl signal wash buffer 1 at 37°C for 3 mins each.

Note: Image the tissue after signal removal to estimate the time required for signal removal. If additional time is necessary, repeat from step 16. The acrylamide gel-based method would require additional time to remove the signal.After signal removal repeat from step 7.

Protocol on automation platform: Total time 8 hrs.

A) Probe preparation

Preparing the primary stock solution (10 pairs of probes: 5µM final volume)

Up to 10 pairs of oligonucleotides were ordered from IDT for one gene, each at a concentration of 100 µM. 100 µl of oligos from each tube were mixed to form a master mix with a final probe concentration of 5 µM in a 2ml microcentrifuge tube (Labselect, Cat No. MCT-001-200). Three to four genes with different hairpin amplifiers (Molecular Instruments) can be designed and tested in a single round of HCR (Choi et al., 2018). The number of genes tested in each round depends on the number of laser lines in the confocal being used. The stock mix of primary probes are stored at -20°C.

Prepare the 20% EC hybridization buffer with probes complementary to the target RNA

Preparation of DNA oligo mix: Add 10 µl of each of the 5 µM DNA oligo mix and adjust the volume to 1000 µl in 20% EC hybridization buffer in 1.5ml microcentrifuge tube (Labselect, Cat No. MCT-001-150).

Prepare the secondary probes with fluorescent tags

Add 5 µl of each H1 and H2 hairpins (Molecular Instruments) separately in 150+150 µl of Amplification buffer in two 200 µl PCR tubes.

Heat at 95°C for 90 secs in a thermocycler and cool down at room temperature in a dark environment for 30 mins. Mix the two tubes together in a 1.5 ml microcentrifuge tube (Labselect, Cat No. MCT-001-150) and use.

Note: The secondaries can be used multiple times. After the reaction, collect them from the secondary collection tube and store at -20°C. For repeated use, heat the secondary probes in amplification buffer at 42°C for 30 mins before use.

B) Steps

Fixation and permeabilization steps (done manually):

1) Dissect the tissue in 1x PBS at room temperature.

2) Transfer the tissue in 500 µl 1x PBST supplemented with 4% formaldehyde and fix for 30-60 mins at room temperature (RT) with shaking. Smaller fixation time is required for thinner tissues while longer time is required for thicker tissues.

4) Wash the tissue 3 times with 500 µl 1x PBST (3mins each) at RT.

5) Add 500 µl of detergent solution or alternative permeabilization buffer and leave the tissue for 30 mins at 37°C.

6) Wash 3 times with 500 µl 1x PBST (3 mins each) at RT.

7) Wash 2 times with 500 µl 5x SSCT (3mins each) at RT.

8) Transfer the sample to a 3.5mm confocal dish (SPL, Cat No. 240202783).

Note: At this step you can either embed the sample in the acrylamide gel mentioned above or perform the experiment with the tissue free-floating in the buffer.

9) Transfer the tissue to 500 µl 30% probe hybridization buffer or 20% EC hybridization buffer at RT.

Note: Tissues can be stored in 30% probe hybridization buffer at 4°C for 2 weeks without any significant loss of signal. Do not store samples in 20% EC hybridization buffer as the solution will crystallize at 4°C.

10) Add all the buffers to separate containers in the micro-fluidics' robot. Signal wash buffer 1 and 2, and signal removal buffer are added after the first cycle of HCR3.0 i.e., for every cycle after the first signal acquisition cycle.

Tube 1 type: 15 ml conical centrifuge tubes (SPL, Cat No. 50015). Total number of tubes: 10.

Tube 2 type: 15 ml amber conical tube (SPL, Cat No. 54015). Total number of tubes: 1.

i) 5x SSCT: 15ml. Tube 1.

ii) 30% probe wash buffer/20% EC Wash buffer: 10 ml. Tube 1.

iii) Amplification buffer: 500 µl. Tube 1.

iv) 20% EC hybridization buffer: 500 µl. Tube 1.

v) 20% EC hybridization buffer with probes: 500 µl. Tube 1.

vi) Secondary fluorescence probes in amplification buffer: 300 µl. Tube 2.

vii) DAPI buffer: 500 µl. Tube 1.

viii) Signal wash buffer 2: 10 ml (only from cycle 2 onwards). Tube 1.

ix) Signal removal buffer: 500 µl (only from cycle 2 onwards). Tube 1.

x) Signal wash buffer 1: 500 µl (only from cycle 2 onwards). Tube 1.

xi) Imaging buffer: 500 µl. Tube 1.

11) Transfer the confocal dish with sample to the arc chamber and make sure the microcomb chip fits perfectly on top of the confocal dish. For the free floating tissue use microcomb combination 1 (**Figure 1D**) and for the acrylamide gel -based methodology use microcomb combination 2 (**Figure 1E**).

12) Turn on the fluidics cycle by pressing the appropriate button (see below).

Buttons in the micro-fluidics' robot:

a) If you are running your first FISH cycle: Press the Cycle 1.0 button. This runs a script that performs the first round of HCR3.0.

b) For every subsequent FISH cycle (which includes signal removal): Press the Cycle 2.0 button. This will run a script that performs every subsequent round of HCR3.0.

c) For quick cleaning: Press Clean1 button. This will execute a script that will flush any remaining buffer or probe in the primary probe tube.

d) For deep cleaning: Press the Clean2 button. This will execute a script to flush any remaining buffer/probes in all the tubes.

13) After each reaction load 1 ml of the robot cleaning solution and either perform quick cleaning to clean the primary probe tube or deep cleaning to clean all the tubing. Deep cleaning is recommended after every multiplexing experiment.

14) Repeat from step 10.

Note: The robot is designed to collect the secondary fluorescent probes in a separate container. The collected probes can be reused 2-3 times (optional). The script can be changed to perform hybridization and washes for other FISH methodologies of choice.

Authors contribution

TDB: Conceptualization, hardware design, coding, methodology (butterfly wings, zebrafish), writing - original draft, writing -review and editing. JR: Methodology (zebrafish), writing – review and editing. ASM: Supervision, writing – review and editing, funding. KHC: Supervision, writing – review and editing, funding. AM: Conceptualization, supervision, funding, writing – review and editing.

Acknowledgement

We thank DBS-CBIS confocal facility for access to the Olympus fv3000 confocal microscope. Shen Tian, Linwan Zhang, and Maurice Lee for helpful tips on the methodology. Kian Long Tan, Suriya Murugeshan, and Shen Tian for productive discussion and proofreading the manuscript.

Funding

This project was supported by Singapore Ministry of Education MOE-T2EP30220-0020 awarded to ASM and NRF-CRP25-2020-0001 awarded to KHC and AM.

Conflict of Interest

A provisional patent involving the arc chamber, and the automation system mentioned in the present methodology has been filed.

Availability of resources

All the data mentioned in the present method are described in the supplementary information.

References

Antinucci, P. and Hindges, R. (2016). A crystal-clear zebrafish for in vivo imaging. *Sci. Rep.* **6**, 1–10.

Banerjee, T. Das and Monteiro, A. (2020a). Molecular mechanisms underlying simplification of venation patterns in holometabolous insects. *Development.*

Banerjee, T. Das and Monteiro, A. (2020b). Dissection of Larval and Pupal Wings of Bicyclus anynana Butterflies. *Methods Protoc.* **3**, 5.

Banerjee, T. Das and Monteiro, A. (2023). Reuse of a wing venation gene-regulatory subnetwork in patterning the eyespot rings of butterflies. *bioRxiv*.

Banerjee, T. Das, Ramos, D. and Monteiro, A. (2020). Expression of multiple engrailed family genes in eyespots of Bicyclus anynana butterflies does not implicate the duplication events in the evolution of this morphological novelty. *Front. Ecol. Evol.* **8**, 1–12.

Banerjee, T. Das, Tian, S. and Monteiro, A. (2022). Laser Microdissection-Mediated Isolation of Butterfly Wing Tissue for Spatial Transcriptomics. *Methods Protoc.*

Banerjee, T. Das, Murugesan, S. N., Connahs, H. and Monteiro, A. (2023). Spatial and temporal regulation of Wnt signaling pathway members in the development of butterfly wing patterns. *Sci. Adv.*

Bruce, H. S., Jerz, G., Kelly, S., McCarthy, J., Pomerantz, A., Senevirathne, G., Sherrard, A., Sun, D. A., Wolff, C. and Patel, N. H. (2021). Hybridization Chain Reaction (HCR) In Situ Protocol. *protocols.io* 1–10.

Çelik, A., Fuss, S. H. and Korsching, S. I. (2002). Selective targeting of zebrafish olfactory receptor neurons by the endogenous OMP promoter. *Eur. J. Neurosci.* **15**, 798–806.

Chatterjee, M., Yu, X. Y., Brady, N. K., Hatto, G. C. and Reed, R. D. (2024). Mirror Determines the Far Posterior Domain in Butterfly Wings. 1–17.

Chen, K. H., Boettiger, A. N., Moffitt, J. R., Wang, S. and Zhuang, X. (2015). Spatially resolved, highly multiplexed RNA profiling in single cells. *Science (80-.).* **348**, 1360–1363.

Chen, A., Liao, S., Cheng, M., Ma, K., Wu, L., Lai, Y., Qiu, X., Yang, J., Xu, J., Hao, S., et al. (2022). Spatiotemporal transcriptomic atlas of mouse organogenesis using DNA nanoball-patterned arrays. *Cell* **185**, 1777-1792.e21.

Choi, H. M. T., Schwarzkopf, M., Fornace, M. E., Acharya, A., Artavanis, G., Stegmaier, J., Cunha, A. and Pierce, N. A. (2018). Third-generation in situ hybridization chain reaction□: multiplexed , quantitative , sensitive , versatile , robust. *Dev.* **1**,.

Choi, J., Li, J., Ferdous, S., Liang, Q., Moffitt, J. R. and Chen, R. (2023). Spatial organization of the mouse retina at single cell resolution by MERFISH. *Nat. Commun.* **14**,.

Codeluppi, S., Borm, L. E., Zeisel, A., La Manno, G., van Lunteren, J. A., Svensson, C. I. and Linnarsson, S. (2018). Spatial organization of the somatosensory cortex revealed by osmFISH. *Nat. Methods* **15**, 932–935.

Connahs, H., Tlili, S., van Creij, J., Loo, T. Y. J., Banerjee, T. Das, Saunders, T. E. and Monteiro, A. (2019a). Distal-less activates butterfly eyespots consistent with a reaction diffusion process. *Development* dev.169367.

Connahs, H., Tlili, S., van Creij, J., Loo, T. Y. J. J., Banerjee, T. Das, Saunders, T. E. and Monteiro, A. (2019b). Activation of butterfly eyespots by Distal-less is consistent with a reaction-diffusion process. *Development* **146**, 1–12.

Coutant, A., Cockenpot, V., Muller, L., Degletagne, C., Pommier, R., Tonon, L., Ardin, M., Michallet, M. C., Caux, C., Laurent, M., et al. (2023). Spatial Transcriptomics Reveal Pitfalls and Opportunities for the Detection of Rare High-Plasticity Breast Cancer Subtypes. *Lab. Investig.* **103**,.

Datta, S., Malhotra, L., Dickerson, R., Chaffee, S., Sen, C. K. and Roy, S. (2015). Laser capture microdissection: Big data from small samples. *Histol. Histopathol.* **30**, 1255–1269.

De Zuani, M., Xue, H., Park, J. S., Dentro, S. C., Seferbekova, Z., Tessier, J., Curras-Alonso, S., Hadjipanayis, A., Athanasiadis, E. I., Gerstung, M., et al. (2024). Single-cell and spatial transcriptomics analysis of non-small cell lung cancer. *Nat. Commun.* **15**,.

Fang, R., Halpern, A. R., Rahman, M. M., Huang, Z., Lei, Z., Hell, S. J., Dulac, C. and Zhuang, X. (2023). Three-dimensional single-cell transcriptome imaging of thick tissues. *Elife*

2023.07.21.550124.

Ficarrotta, V., Hanly, J. J., Loh, L. S., Francescutti, C. M., Ren, A., Tunström, K., Wheat, C. W., Porter, A. H., Counterman, B. A. and Martin, A. (2022). A genetic switch for male UV iridescence in an incipient species pair of sulphur butterflies. *Proc. Natl. Acad. Sci. U. S. A.* **119**,.

Filippi, A., Mueller, T. and Driever, W. (2014). vglut2 and gad expression reveal distinct patterns of dual GABAergic versus glutamatergic cotransmitter phenotypes of dopaminergic and noradrenergic neurons in the zebrafish brain. *J. Comp. Neurol.* **522**, 2019–2037.

Funakoshi, Y., Minami, M. and Tabata, T. (2001). mtv shapes the activity gradient of the Dpp morphogen through regulation of thickveins. *Development* **128**, 67–74.

Gandin, V., Kim, J., Yang, L.-Z., Lian, Y., Kawase, T., Hu, A., Rokicki, K., Fleishman, G., Tillberg, P., Castrejon, A. A., et al. (2024). Deep-Tissue Spatial Omics: Imaging Whole-Embryo Transcriptomics and Subcellular Structures at High Spatial Resolution. *bioRxiv* 2024.05.17.594641.

Gemmer, A., Mirkes, K., Anneser, L., Eilers, T., Kibat, C., Mathuru, A., Ryu, S. and Schuman, E. (2022). Oxytocin receptors influence the development and maintenance of social behavior in zebrafish (Danio rerio). *Sci. Rep.* **12**, 1–13.

Gerlai, R. (2020). Evolutionary conservation, translational relevance and cognitive function: The future of zebrafish in behavioral neuroscience. *Neurosci. Biobehav. Rev.* **116**, 426–435.

Goh, J. J. L., Chou, N., Seow, W. Y., Ha, N., Cheng, C. P. P., Chang, Y. C., Zhao, Z. W. and Chen, K. H. (2020). Highly specific multiplexed RNA imaging in tissues with split-FISH. *Nat. Methods* **17**, 689–693.

Guichard, a, Biehs, B., Sturtevant, M. a, Wickline, L., Chacko, J., Howard, K. and Bier, E. (1999). rhomboid and Star interact synergistically to promote EGFR/MAPK signaling during Drosophila wing vein development. *Development* **126**, 2663–2676.

Hanly, J. J., Wallbank, R. W. R., McMillan, W. O. and Jiggins, C. D. (2019). Conservation and flexibility in the gene regulatory landscape of heliconiine butterfly wings. *Evodevo* **10**, 1–14.

Hanly, J. J., Loh, L. S., Mazo-Vargas, A., Rivera-Miranda, T. S., Livraghi, L., Tendolkar, A., Day, C. R., Liutikaite, N., Earls, E. A., Corning, O. B. W. H., et al. (2023). Frizzled2 receives WntA signaling during butterfly wing pattern formation. *Dev.* **150**,.

He, S., Bhatt, R., Birditt, B., Brown, C., Brown, E., Chantranuvatana, K., Danaher, P., Dunaway, D., Filanoski, B. and Garrison, R. G. (2021). High-plex multiomic analysis in FFPE tissue at single-cellular and subcellular resolution by spatial molecular imaging. *bioRxiv* 2011–2021.

Jung, N. and Kim, T. K. (2023). Spatial transcriptomics in neuroscience. *Exp. Mol. Med.* **55**, 2105–2115.

Kalinka, A., Myśliwy, M. and Achrem, M. (2020). Comparison of ethylene carbonate and formamide as components of the hybridization mixture in fish. *Sci. Agric.* **78**, 1–5.

Keys, D. N., Lewis, D. L., Selegue, J. E., Pearson, B. J., Goodrich, L. V., Johnson, R. L., Gates, J., Scott, M. P. and Carroll, S. B. (1999). Recruitment of a hedgehog Regulatory Circuit in Butterfly Eyespot Evolution. *Science (80-.).* **283**, 532–534.

Kishi, J. Y., Lapan, S. W., Beliveau, B. J., West, E. R., Zhu, A., Sasaki, H. M., Saka, S. K., Wang, Y., Cepko, C. L. and Yin, P. (2019). SABER amplifies FISH: enhanced multiplexed imaging of RNA and DNA in cells and tissues. *Nat. Methods* **16**, 533–544.

Kuan, Y. S., Yu, H. H., Moens, C. B. and Halpern, M. E. (2007). Neuropilin asymmetry mediates a left-right difference habenular connectivity. *Development* **134**, 857–865.

Liu, L., Liu, C., Quintero, A., Wu, L., Yuan, Y., Wang, M., Cheng, M., Leng, L., Xu, L., Dong, G., et al. (2019). Deconvolution of single-cell multi-omics layers reveals regulatory heterogeneity. *Nat. Commun.* **10**,.

Liu, J., Tran, V., Naga, V., Vemuri, P., Byrne, A., Agarwal, S., Wang, R., Awayan, K., Murti, A., Aris Taychameekiatchai, B. W., et al. (2022). Comparative analysis of MERFISH spatial transcriptomics with bulk and single-cell RNA sequencing. *bioRxiv*.

Lubeck, E. and Cai, L. (2012). Single-cell systems biology by super-resolution imaging and combinatorial labeling. *Nat. Methods* **9**, 743–748.

Martin, A. and Reed, R. D. (2010). wingless and aristaless2 define a developmental ground plan for moth and butterfly wing pattern evolution. *Mol. Biol. Evol.* **27**, 2864–2878.

Martin, A. and Reed, R. D. (2014). Wnt signaling underlies evolution and development of the butterfly wing pattern symmetry systems. *Dev. Biol.* **395**, 367–378.

Matsuoka, Y. and Monteiro, A. (2022). Ultrabithorax modifies a regulatory network of genes essential for butterfly eyespot development in a wing sector-specific manner . *Development*.

Matthiesen, S. H. and Hansen, C. M. (2012). Fast and non-toxic in situ hybridization without blocking of repetitive sequences. *PLoS One* **7**, 1–8.

Mazo-vargas, A., Concha, C., Livraghi, L., Massardo, D., Wallbank, R. W. R. and Zhang, L. (2017). Macroevolutionary shifts of WntA function potentiate butterfly wing-pattern diversity. *PNAS* **114**, 10701–10706.

Moffitt, J. R., Hao, J., Wang, G., Chen, K. H., Babcock, H. P. and Zhuang, X. (2016a). High-throughput single-cell gene-expression profiling with multiplexed error-robust fluorescence in situ hybridization. *Proc. Natl. Acad. Sci. U. S. A.* **113**, 11046–11051.

Moffitt, J. R., Hao, J., Bambah-Mukku, D., Lu, T., Dulac, C. and Zhuang, X. (2016b). High-performance multiplexed fluorescence in situ hybridization in culture and tissue with matrix imprinting and clearing. *Proc. Natl. Acad. Sci. U. S. A.* **113**, 14456–14461.

Moffitt, J. R., Bambah-Mukku, D., Eichhorn, S. W., Vaughn, E., Shekhar, K., Perez, J. D., Rubinstein, N. D., Hao, J., Regev, A., Dulac, C., et al. (2018). Molecular, spatial, and functional single-cell profiling of the hypothalamic preoptic region. *Science (80-.).* **362**,.

Monteiro, A., Glaser, G., Stockslager, S., Glansdorp, N. and Ramos, D. (2006). Comparative insights into questions of lepidopteran wing pattern homology. *BMC Dev. Biol.* **6**, 52.

Mueller, T. and Wullimann, M. F. (2002). Expression domains of neuroD (nrd) in the early postembryonic zebrafish brain. *Brain Res. Bull.* **57**, 377–379.

Neumann, C. J. and Cohen, S. M. (1997). Long-range action of Wingless organizes the dorsal-ventral axis of the Drosophila wing. *Development* **124**, 871–880.

Nichterwitz, S., Chen, G., Aguila Benitez, J., Yilmaz, M., Storvall, H., Cao, M., Sandberg, R., Deng, Q. and Hedlund, E. (2016). Laser capture microscopy coupled with Smart-seq2 for precise spatial transcriptomic profiling. *Nat. Commun.* **7**, 1–11.

Nichterwitz, S., Nijssen, J., Storvall, H., Schweingruber, C., Comley, L. H., Allodi, I., Van Der Lee, M., Deng, Q., Sandberg, R. and Hedlund, E. (2020). LCM-seq reveals unique transcriptional adaptation mechanisms of resistant neurons and identifies protective pathways in spinal muscular atrophy. *Genome Res.* **30**, 1083–1096.

Oliver, J. C., Tong, X. L., Gall, L. F., Piel, W. H. and Monteiro, A. (2012). A Single Origin for Nymphalid Butterfly Eyespots Followed by Widespread Loss of Associated Gene Expression. *PLoS Genet.* **8**,.

Phillips, R. G., Roberts, I. J., Ingham, P. W. and Whittle, J. R. (1990). The Drosophila segment polarity gene patched is involved in a position-signalling mechanism in imaginal discs. *Development* **110**, 105–114.

Prakash, A., Dion, E., Banerjee, T. Das and Monteiro, A. (2024). The molecular basis of scale development highlighted by a single-cell atlas of Bicyclus anynana butterfly pupal forewings. *Cell Rep.* **43**,.

Raine, J., Kibat, C., Banerjee, T. Das, Mathuru, A. S. and Biology, C. (2024). chrna3 modulates biphasic response to alcohol. *bioRxiv*.

Rao, A., Barkley, D., França, G. S. and Yanai, I. (2021). Exploring tissue architecture using spatial transcriptomics. *Nature* **596**, 211–220.

Reed, R. D. and Gilbert, L. E. (2004). Wing venation and Distal-less expression in Heliconius butterfly wing pattern development. 628–634.

Reed, R. D. and Serfas, M. S. (2004). Butterfly Wing Pattern Evolution Is Associated with Changes in a Notch/Distal-less Temporal Pattern Formation Process. *Curr. Biol.* **14**, 1159–1166.

Reed, R. D., Chen, P. H. and Frederik Nijhout, H. (2007). Cryptic variation in butterfly eyespot development: The importance of sample size in gene expression studies. *Evol. Dev.* **9**, 2–9.

Reed, R. D., Papa, R., Martin, A., Hines, H. M., Kronforst, M. R., Chen, R., Halder, G., Nijhout, H. F. and Mcmillan, W. O. (2011). optix Drives the Repeated Convergent Evolution of Butterfly Wing Pattern Mimicry. *Science (80-.).* **333**, 1137–1141.

Reed, R. D., Selegue, J. E., Zhang, L. and Brunetti, C. R. (2020). Transcription factors underlying wing margin color patterns and pupal cuticle markings in butterflies. *Evodevo* **11**, 1–10.

Rodriques, S. G., Stickels, R. R., Goeva, A., Martin, C. A., Murray, E., Vanderburg, C. R., Welch, J., Chen, L. M., Chen, F. and Macosko, E. Z. (2019). Slide-seq: A scalable technology for measuring genome-wide expression at high spatial resolution. *Science (80-.).* **363**, 1463–1467.

Saenko, S. V., Marialva, M. S. P. P. and Beldade, P. (2011). Involvement of the conserved Hox gene Antennapedia in the development and evolution of a novel trait. *Evodevo* **2**, 9.

Saliba, A. E., Westermann, A. J., Gorski, S. A. and Vogel, J. (2014). Single-cell RNA-seq: Advances and future challenges. *Nucleic Acids Res.* **42**, 8845–8860.

Schindelin, J., Arganda-Carreras, I., Frise, E., Kaynig, V., Longair, M., Pietzsch, T., Preibisch, S., Rueden, C., Saalfeld, S., Schmid, B., et al. (2012). Fiji: An open-source platform for biological-image analysis. *Nat. Methods* **9**, 676–682.

Schulte, S. J., Fornace, M. E., Hall, J. K., Shin, G. J. and Pierce, N. A. (2024). HCR spectral imaging: 10-plex, quantitative, high-resolution RNA and protein imaging in highly autofluorescent samples. *Dev.* **151**,.

Schulze, L., Zada, D. and Lovett-Barron, M. (2023). A medley of gene expression adds new depth to zebrafish brain maps. *Sci. Adv.* **9**, 9–10.

Shah, S., Lubeck, E., Zhou, W. and Cai, L. (2016). In Situ Transcription Profiling of Single Cells Reveals Spatial Organization of Cells in the Mouse Hippocampus. *Neuron* **92**, 342–357.

Shalek, A. K., Satija, R., Shuga, J., Trombetta, J. J., Gennert, D., Lu, D., Chen, P., Gertner, R. S., Gaublomme, J. T., Yosef, N., et al. (2014). Single-cell RNA-seq reveals dynamic paracrine control of cellular variation. *Nature* **510**, 363–369.

Ståhl, P. L., Salmén, F., Vickovic, S., Lundmark, A., Navarro, J. F., Magnusson, J., Giacomello, S., Asp, M., Westholm, J. O., Huss, M., et al. (2016). Visualization and analysis of gene expression in tissue sections by spatial transcriptomics. *Science (80-.).* **353**, 78–82.

Sternson, I. S., Chase, C., Yang, H. and Chase, C. (2022). MATERIALS AND METHODS FOR SERIAL MULTIPLEXED DETECTION OF RNA IN CELLS AND TISSUES. **2**,.

Tian, S., Asano, Y., Banerjee, T. Das, Komata, S., Liang, J., Wee, Q., Lamb, A., Wang, Y., Murugesan, S. N., Fujiwara, H., et al. (2024). A microRNA is the effector gene of a classic evolutionary hotspot locus. *Science (80-.).* **1141**, 1135–1141.

Unger, J. L. and Glasgow, E. (2003). Expression of isotocin-neurophysin mRNA in developing zebrafish. *Gene Expr. Patterns* **3**, 105–108.

Valdeolivas, A., Amberg, B., Giroud, N., Richardson, M., Gálvez, E. J. C., Badillo, S., Julien-Laferrière, A., Túrós, D., Voith von Voithenberg, L., Wells, I., et al. (2024). Profiling the heterogeneity of colorectal cancer consensus molecular subtypes using spatial transcriptomics. *npj Precis. Oncol.* **8**,.

Wang, F., Flanagan, J., Su, N., Wang, L. C., Bui, S., Nielson, A., Wu, X., Vo, H. T., Ma, X. J. and Luo, Y. (2012). RNAscope: A novel in situ RNA analysis platform for formalin-fixed, paraffin-embedded tissues. *J. Mol. Diagnostics* **14**, 22–29.

Wang, X., Allen, W. E., Wright, M. A., Sylwestrak, E. L., Samusik, N., Vesuna, S., Evans, K., Liu, C., Ramakrishnan, C., Liu, J., et al. (2018). Three-dimensional intact-tissue sequencing of single-cell transcriptional states. *Science (80-.).* **361**,.

Wang, Y., Eddison, M., Fleishman, G., Weigert, M., Xu, S., Wang, T., Rokicki, K., Goina, C., Henry, F. E., Lemire, A. L., et al. (2021). EASI-FISH for thick tissue defines lateral hypothalamus spatio-molecular organization. *Cell* **184**, 6361-6377.e24.

Wee, J. L. Q., Das Banerjee, T., Prakash, A., Seah, K. S. and Monteiro, A. (2022). Distal-less and spalt are distal organisers of pierid wing patterns. *Evodevo* **13**, 1–14.

Wu, S. Z., Al-Eryani, G., Roden, D. L., Junankar, S., Harvey, K., Andersson, A., Thennavan, A., Wang, C., Torpy, J. R., Bartonicek, N., et al. (2021a). A single-cell and spatially resolved atlas of human breast cancers. *Nat. Genet.* **53**, 1334–1347.

Wu, R., Guo, W., Qiu, X., Wang, S., Sui, C., Lian, Q., Wu, J., Shan, Y., Yang, Z., Yang, S., et al. (2021b). Comprehensive analysis of spatial architecture in primary liver cancer. *Sci. Adv.* **7**,.

Wu, L., Yan, J., Bai, Y., Chen, F., Zou, X., Xu, J., Huang, A., Hou, L., Zhong, Y., Jing, Z., et al. (2023). An invasive zone in human liver cancer identified by Stereo-seq promotes hepatocyte–tumor cell crosstalk, local immunosuppression and tumor progression. *Cell Res.* **33**, 585–603.

Zhang, M., Eichhorn, S. W., Zingg, B., Yao, Z., Cotter, K., Zeng, H., Dong, H. and Zhuang, X. (2021). Spatially resolved cell atlas of the mouse primary motor cortex by MERFISH. *Nature* **598**, 137–143.

Zhang, Q., Abdo, R., Iosef, C., Kaneko, T., Cecchini, M., Han, V. K. and Li, S. S. C. (2022). The spatial transcriptomic landscape of non-small cell lung cancer brain metastasis. *Nat. Commun.* **13**,.

Zhou, X., Seow, W. Y., Ha, N., Cheng, T. H., Lingfan, J., Boonruangkan, J., Jie, J., Goh, L., Prabhakar, S., Chou, N., et al. (2023a). Highly sensitive spatial transcriptomics using FISHnCHIPs of multiple co-expressed genes. *Nat. Commun.* 2023.04.11.536345.

Zhou, P. Y., Zhou, C., Gan, W., Tang, Z., Sun, B. Y., Huang, J. L., Liu, G., Liu, W. R., Tian, M. X., Jiang, X. F., et al. (2023b). Single-cell and spatial architecture of primary liver cancer. *Commun. Biol.* **6**, 1–17.

A
Dissection
Bicyclus anynana wing
Danio rerio larva
B
Fixation+Permeablization
OR
C
Hybridization and washes
Mounting + Imaging
Remove coverslip
and move tissue to wells/tubes
Gene Set 1
Gene Set 1
Gene Set 1
OR
Remove signal
Free floating manual multiplexing: (36-48 hrs using fromamide)
(20-24 hrs using ethylene carbonate)
D
Acrylamide gel embedding
Hybridization and washes
Imaging
Remove signal
Gel based manual multiplexing:
48-60 hrs using formamide
30-36 hrs using ethylene carbonate
E
Free floating
Add sample in microcomb part 1
Remove sample from slide, remove signal, and repeat hybridization
Install part 2
and
Arc chamber
Mounting + Imaging
Gene Set 1
Gene Set 1
F
Gel based
Fix sample in gel
Add part 1
Install part 2
and
Arc chamber
Run experiment in automation system
Imaging in confocal dish
Remove signal and repeat hybridization
Automation based multiplexing (8-10 hrs)
G
Primary probes
Secondary probes
Amplification (HCR)
Imaging
Signal removal
Remove primary and secondary probes
Repeat N number of cycles

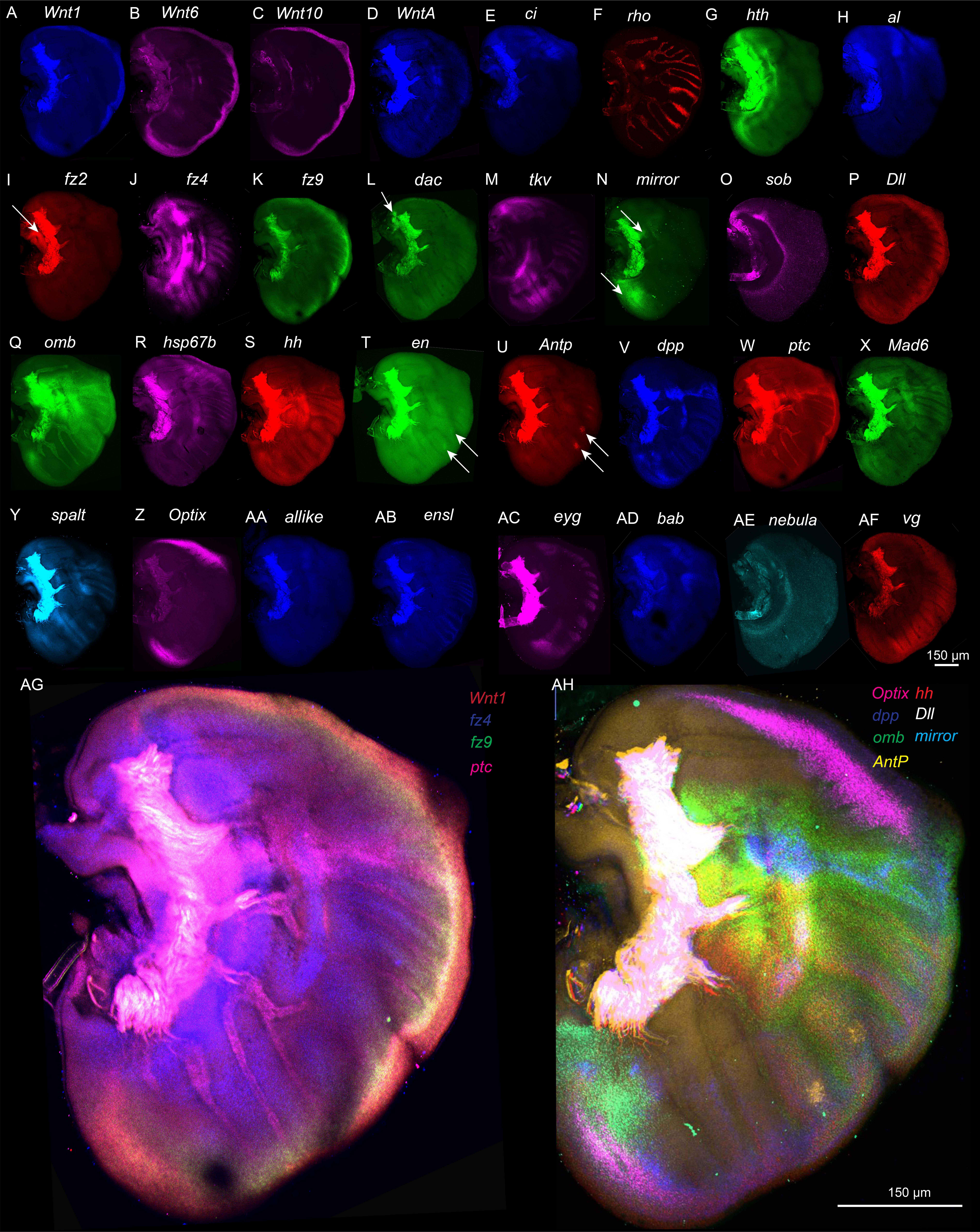
A Wnt1
B Wnt6
C Wnt10
D WntA
E ci
F rho
G hth
H al
I fz2
J fz4
K fz9
L dac
M tkv
N mirror
O sob
P Dll
Q omb
R hsp67b
S hh
T en
U Antp
V dpp
W ptc
X Mad6
Y spalt
Z Optix
AA allike
AB ensl
AC eyg
AD bab
AE nebula
AF vg
150 µm
AG
Wnt1
fz4
fz9
ptc
AH
Optix hh
dpp Dll
omb mirror
AntP
150 µm

A Wnt1
B Wnt6
C Wnt10
D WntA
E ci
F rho
G hth
H al
I fz2
J fz4
K fz9
L dac
M tkv
N mirror
O sob
P Dll
Q omb
R hsp67b
S hh
T AntP
U dpp
V patched
W Mad6
X Notch
Y spalt
Z Optix
AA al-like
AB ensl
AC eyg
AD bab
AE nebula
AF vg
200 µm
AG
hsp67b
rho
omb
100 µm
AH
Optix hh
dpp Antp
omb fz9
ci
100 µm

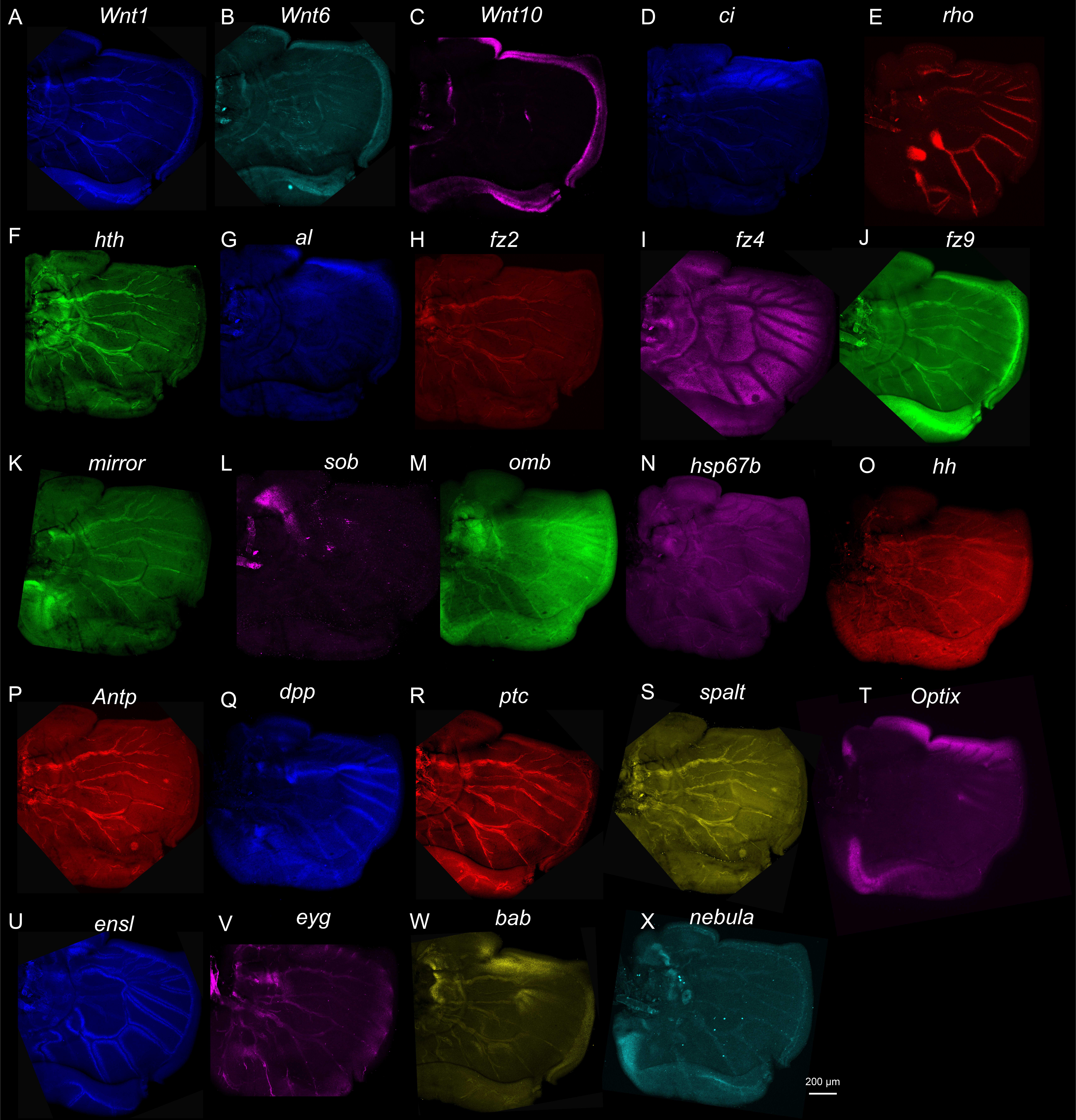
A
Wnt1
B
Wnt6
C
Wnt10
D
ci
E
rho
F
hth
G
al
H
fz2
I
fz4
J
fz9
K
mirror
L
sob
M
omb
N
hsp67b
O
hh
P
Antp
Q
dpp
R
ptc
S
spalt
T
Optix
U
ensl
V
eyg
W
bab
X
nebula
200 μm

A Wnt1
B Wnt6
C WntA
D al
E fz4
F fz9
G dac
H tkv
I mirror
J sob
K Dll
L omb
M hh
N Antp
O dpp
P ptc
Q Mad6
R spalt
S Optix
T bab
U ensl
V al-like
W eyg
X vg
200 µm
Y
Optix
omb
dpp
hh
Z
Wnt6
dac
al
tkv
fz9
spalt
ptc
100 µm

A
Wnt1
B
Wnt6
C
Wnt10
D
WntA
ci
E
E’
90 µm
F
hth
G
fz2
H
fz4
I
fz9
J
dac
K
tkv
L
Dll
M
omb
N
hh
O
en
P
Antp
Q
dpp
R
ptc
S
Notch
T
spalt
U
Optix
V
bab
W
vg
180 µm

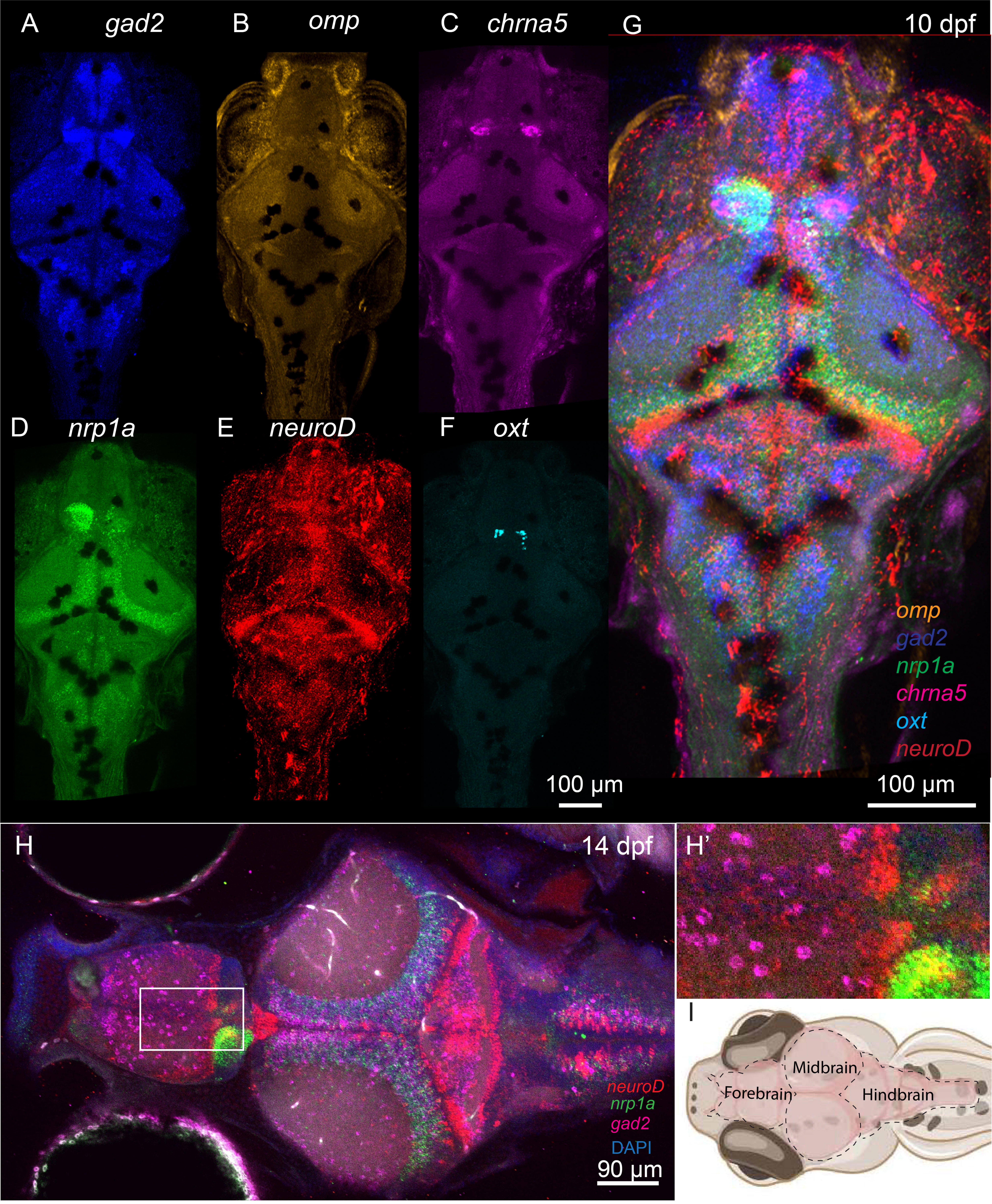
A gad2
B omp
C chrna5
G
10 dpf
D nrp1a
E neuroD
F oxt
omp
gad2
nrp1a
chrna5
oxt
neuroD
100 μm
100 μm
H
14 dpf
neuroD
nrp1a
gad2
DAPI
90 μm
H'
I
Midbrain
Forebrain
Hindbrain